

N92-33599

Unclass

G3/25 0117778

(NASA-CR-190743) THEORETICAL
INVESTIGATION OF GAS-SURFACE
INTERACTIONS Progress Report, 1
Nov. 1991 - 31 Jul. 1992 (Eloret
Corp.) 67 p

THEORETICAL INVESTIGATION OF GAS - SURFACE INTERACTIONS

*AMES
IN-25-CR
117778
P, 67*

Periodic Research Report
Cooperative Agreement NCC2-552

for the period
November 1, 1991 - July 31, 1992

Submitted to

National Aeronautics and Space Administration
Ames Research Center
Moffett Field, California 94035

Computational Chemistry Branch
Dr. Stephen R. Langhoff, Chief and Technical Monitor

Thermosciences Division
Dr. Jim Arnold, Chief

Prepared by

ELORET INSTITUTE
1178 Maraschino Drive
Sunnyvale, CA 94087
Phone: 408 730-8422 and 415 493-4710
Fax: 408 730-1441

K. Heinemann, President and Grant Administrator
Kenneth G. Dyllal, Principal Investigator

16 September, 1992

1. The first part of the document is a list of names and addresses.

2

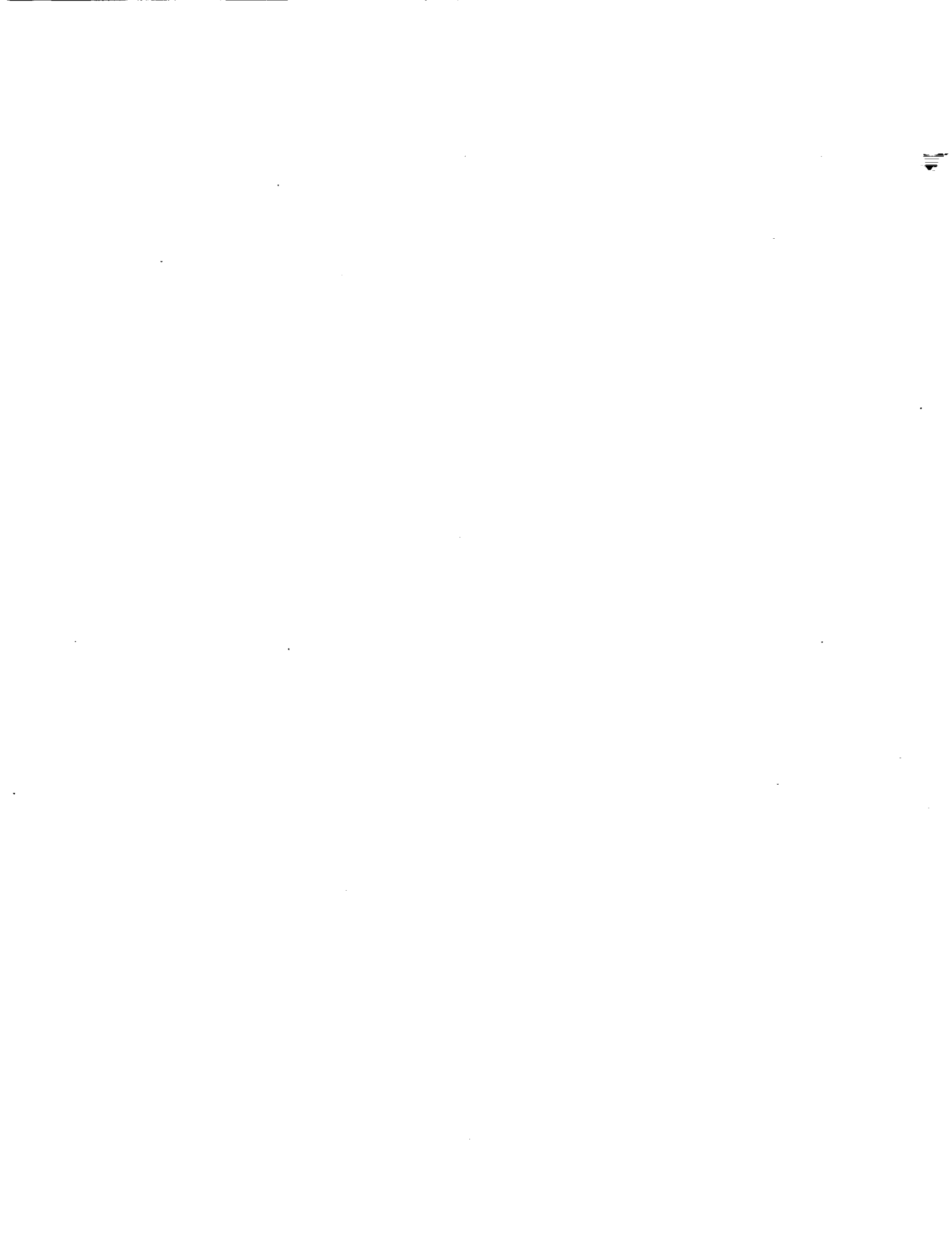
3

SUMMARY

The investigation into the appearance of intruder states from the negative continuum when some of the two-electron integrals involving the small component of the wave function were omitted has been completed and published [1]. The work shows that provided all integrals involving core contracted functions in an atomic general contraction are included, or that the core functions are radially localized, meaningful results are obtained and intruder states do not appear. Reprints of the paper are attached.

In the area of program development, the Dirac-Hartree-Fock (DHF) program for closed-shell polyatomic molecules has been extended to permit Kramers-restricted open-shell DHF calculations with one electron in an open shell or one hole in a closed shell, or state-averaged DHF calculations over several particle or hole doublet states. Code for two open shells is still being tested, as is code for limited MCSCF, for situations where the ground state at the DHF level cannot be described by a single determinant, but is a linear combination of a few determinants related by double excitations from one Kramers pair into another. One application of the open-shell code was to the KO molecule [2]. Preprints of this paper are attached.

Another major area of program development which is under development is the transformation of integrals from the scalar basis in which they are generated to the 2-spinor basis employed in parts of the DHF program, and thence to supermatrix form. The reason for these developments is that the DHF program, while written efficiently for the circumstances under which it was expected to be used, is not the most efficient implementation possible. The code was



originally developed under the assumption that disk space would not be available to sort and transform the integrals, and therefore the unordered integrals would have to be used in the construction of the Fock matrix. With the experience gained over the past year, particularly concerning the omission of small component integrals, and with the increase in availability of disk space, it is now possible to consider transforming the integrals. The use of ordered integrals, either in the scalar basis or in the 2-spinor basis, would considerably speed up the construction of the Fock matrix, and even more so if supermatrices were constructed. Furthermore, in order to proceed beyond the SCF level and include electron correlation it is necessary to transform the integrals to the molecular 4-spinor basis. Therefore, a considerable amount of effort has been spent on analyzing the integral ordering and transformation for the DHF problem. Much of this work was used in preparation for the NATO Advanced Summer Institute in Vancouver, BC, in August 1992.

The work of assessing the reliability of the relativistic effective core potentials (RECPs) available in the literature has been continued with calculations on the group IV monoxides. The perturbation of the metal atom provided by oxygen is expected to be larger than that provided by hydrogen and thus provide a better test of the quality of the RECPs. The results of this study have been submitted for publication, and preprints are attached [3].

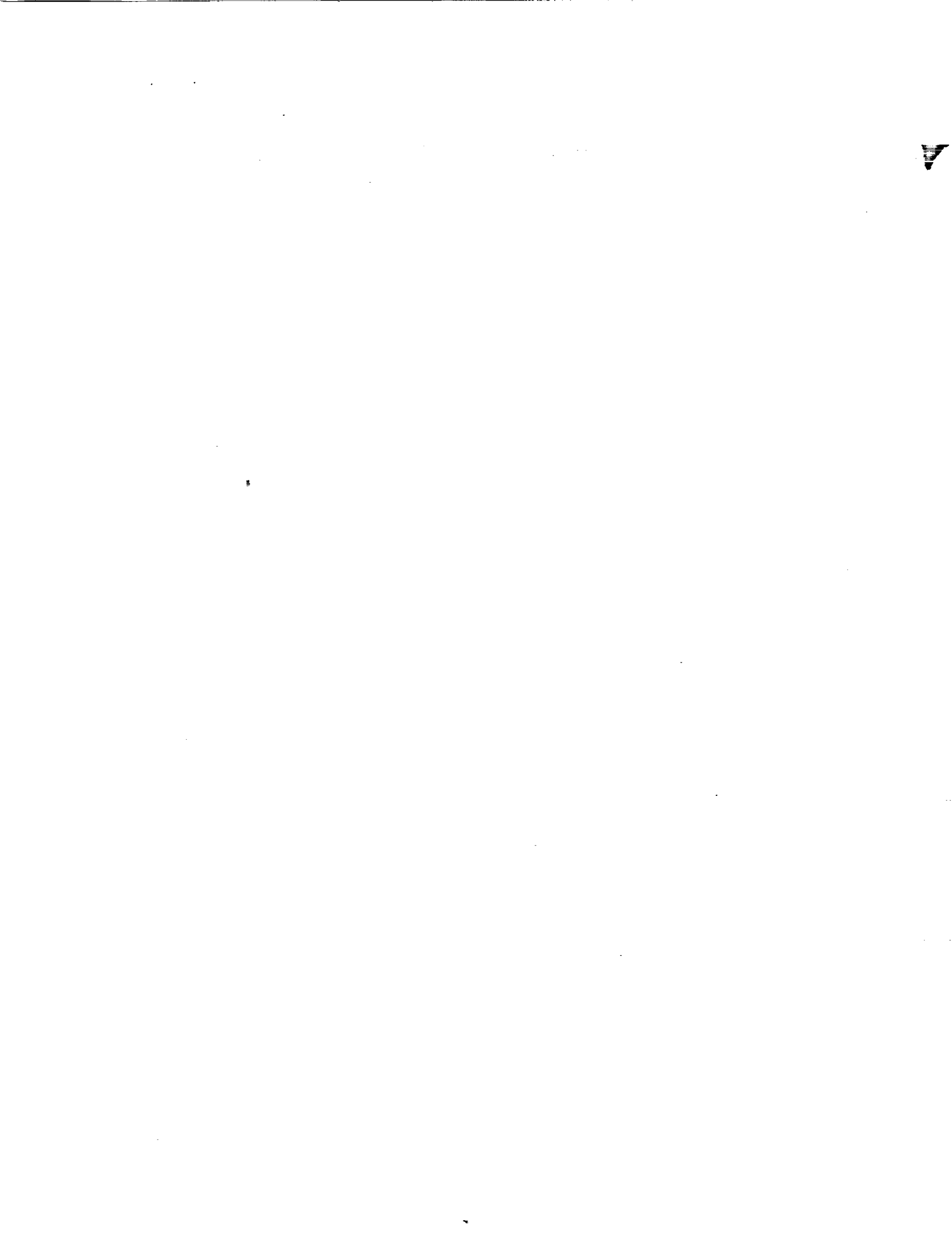
Calculations on the platinum hydrides PtH, PtH⁺ and PtH₂ have been carried out at the nonrelativistic (NR), perturbation theory (PT) and DHF levels. The DHF calculations employed the new open-shell code described above. Geometries, dipole moments, harmonic frequencies, infrared intensities and disso-



ciation energies have been calculated. For purposes of separating spin-orbit effects from the non-fine-structure effects and for determining the validity of the first-order PT approximation, it is proposed to include in the results for the platinum hydrides calculations with the spin-free no-pair code of Hess [4]. A preliminary draft of the paper without these calculations is attached. These results were presented at the West Coast Theoretical Chemistry Conference, held in May 1992 at Pacific Northwest Laboratory.

REFERENCES

- [1] K. G. Dyall, Chem. Phys. Lett. 196, 178 (1992).
- [2] C. W. Bauschlicher, H. Partridge and K. G. Dyall, Chem. Phys. Lett., in press.
- [3] K. G. Dyall, J. Chem. Phys., submitted.
- [4] B. A. Hess, Phys. Rev. A 33, 3742 (1986).



Negative-energy states in the Dirac–Hartree–Fock problem: the effect of omission of two-electron integrals involving the small component

Kenneth G. Dyall

Eloret Institute, 3788 Fabian Way, Palo Alto, CA 94303, USA

Received 12 May 1992

The effect of omission of two-electron integrals involving basis functions for the small component of the wavefunction on the eigenvalue spectrum in the Dirac–Hartree–Fock problem is studied. From an analysis of the Fock matrix it is shown that omission of these integrals moves the negative-energy states down, not up. Their complete omission does not give rise to intruder states. The appearance of intruder states occurs when only some of the core integrals are omitted, due to the nature of particular contraction schemes used for the core basis functions. Use of radially localized functions rather than atomic functions alleviates the intruder state problem.

In a recent paper [1], the effect of the omission of two-electron integrals involving four small-component basis functions in Dirac–Hartree–Fock (DHF) calculations on some properties of PbH_4 was investigated. The reason for the omission was a desire to reduce the large number of integrals involving the small component to a more manageable size. The justification for the omission was that these integrals only contribute to the energy at order α^4 (α is the fine-structure constant), and the contribution is mainly to the core energy. Since the effect on these properties was found to be small, a subsequent DHF study of the molecular properties of the group IV hydrides [2] omitted them entirely. The negative energy spectrum was ignored in these studies. In current work on PbO , the effect of successively adding the $(\text{SS}|\text{SS})$ ^{#1} core integrals from the Pb $n=1, 2$ and 3 shells was investigated. These integrals are few in number and their inclusion should recover most of the energetic effect of the $(\text{SS}|\text{SS})$ integrals. However, in the course of this study, it was found that the

highest negative energy state was increasing in energy as more $(\text{SS}|\text{SS})$ integrals were added, and entering the region of the positive energy states. This observation prompted the present investigation, to understand why, contrary to intuition, the negative energy states moved up as more $(\text{SS}|\text{SS})$ integrals were added, and why they crossed into the region of the positive energy states, above $-2mc^2$ ^{#2}.

It is helpful in this context to consider the “negative energy” states – those with eigenvalues normally below $-2mc^2$ – as positive kinetic energy states for positrons: their energies are then $-(\epsilon + 2mc^2)$, where ϵ is the eigenvalue. This is in line with the interpretation of the Dirac negative energy states from quantum electrodynamics (QED) [3]. The assumption that the addition of the $(\text{SS}|\text{SS})$ integrals should make the negative energy states go down is based on the effect of the integrals on the electron (“positive energy”) states, which is to increase the repulsion, making the electron distribution more diffuse and thereby decreasing the attraction for positrons. While this argument is correct, the reduced at-

Correspondence to: K.G. Dyall, NASA Ames Research Center, MS RTC 230-3, Moffett Field, CA 94035-1000, USA.

^{#1} The notation indicates that each basis function belongs to a given component type, L or S for large or small.

^{#2} The electron rest energy has been subtracted, so that the zero of energy corresponds to the nonrelativistic definition of a free electron with zero kinetic energy.

1

2

3

4

5

6

7

8

Table 1

Effect of addition of (LL|SS) and (SS|SS) integrals and of contraction on the highest positron eigenvalue for Hg^{78+} . Value is given in E_h relative to $-2mc^2$; basis set is tightest 14 s functions from 22s16p13d8f set of ref. [4]

Integrals added	Fully contracted	Half-contracted	Uncontracted
(LL LL)	-12115	-583.16	-580.71
(LL SS)	-12009	-572.19	-569.75
(SS SS)	-12004	-571.06	-568.63

traction is not the major effect. This can be seen by examining the contribution the (SS|SS) integrals make to the Fock matrix. It is sufficient here to consider the case where there is only one occupied spinor and one basis function for each of the large and small components, χ^L and χ^S . The two resultant spinors can be written

$$\psi^e = \begin{pmatrix} a\chi^L \\ b\chi^S \end{pmatrix}, \quad \psi^p = \begin{pmatrix} -b\chi^L \\ a\chi^S \end{pmatrix}, \quad (1)$$

where the superscripts indicate the electron and positron states respectively, and a and b are the coefficients, $a = \mathcal{O}(\alpha^0)$, $b = \mathcal{O}(\alpha^1)$. The diagonal elements of the Fock matrix can be written

$$F_{ee} = \langle \psi^e | h_D | \psi^e \rangle + (\psi^e \psi^e | \psi^e \psi^e),$$

$$F_{pp} = \langle \psi^p | h_D | \psi^p \rangle + (\psi^p \psi^p | \psi^e \psi^e). \quad (2)$$

If we assume that a and b have been determined with the (SS|SS) integral(s) omitted, and consider the contribution the addition of the (SS|SS) integrals makes to the diagonal elements of \mathbf{F} , we arrive at

$$\Delta F_{ee} = b^4 (\chi^S \chi^S | \chi^S \chi^S),$$

$$\Delta F_{pp} = a^2 b^2 (\chi^S \chi^S | \chi^S \chi^S). \quad (3)$$

Table 2

Effect of addition of (LL|SS) and (SS|SS) integrals on the highest positron eigenvalue for Hg as a function of the number of electrons. Value is given in E_h relative to $-2mc^2$; basis set is taken from the 22s16p13d8f set of ref. [4]

Number of electrons	Eigenvalue			Change in eigenvalue		
	(LL LL)	+(LL SS)	+(SS SS)	+(LL SS)	+(SS SS)	total
2	-24.181	-23.637	-23.581	0.544	0.056	0.600
4	-24.181	-23.051	-22.982	1.130	0.069	1.199
10	-24.181	-21.289	-21.184	2.892	0.105	2.997
18	-24.181	-18.909	-18.786	5.272	0.123	5.395

Both contributions are positive, but the diagonal element for the positron state moves upwards by $\mathcal{O}(c^2)$ more than the diagonal element for the electron state. What has been added is an important *attractive* term for the positron states. When the (SS|SS) integrals are added, the potential is changed, increasing the repulsion for the electron states and increasing the attraction for the positron states. The same is true for the (LL|SS) integrals.

As a numerical illustration of the effect discussed above, the Hg^{78+} ion is considered. The tightest 14 s functions were taken from Fægri's [4] 22s16p13d8f set, and fully contracted to give the results in the first column of table 1, where the increase in the positron eigenvalue as the (SS|SS) integrals are added is clearly seen. The increase for the electron eigenvalue is $0.5 E_h$, compared to $5 E_h$ for the positron eigenvalue. That the effect is due to increased positron-electron attraction is demonstrated in table 2, where a series of calculations with an uncontracted basis set for Hg [4] with increasing numbers of electrons is presented. The highest positron eigenvalue increases by $0.6 E_h$ per electron pair as the interaction is turned on. Most of it comes from the (LL|SS) integrals. However, at this rate, the increase for neutral Hg would be insufficient to make the eigenvalue go above $-2mc^2$. Note also that the highest positron eigenvalue is independent of the number of electrons when only the (LL|LL) integrals are included: it is essentially experiencing only the bare nuclear potential, since the contributions of the (LL|LL) integrals to it are $\mathcal{O}(\alpha^4)$. Neither of these illustrations showed any sign of the intruder states noticed for PbO, and on the basis of the above arguments, the omission of (SS|SS) integrals should cause a downward movement of the positron eigenvalues, not upward.

Basis set contraction is one possible source of problems in the positron spectrum. If the core is heavily contracted, the small-component functions will not be very suitable for describing scattering states. The positron states closest to $-2mc^2$ are composed of the most diffuse basis functions, however, so that contraction of the core should not greatly influence these states. In the lower region of the positron spectrum, contraction will decrease the number of basis functions describing the region, giving a sparser discrete representation of the scattering states, and thus shifting the highest positron eigenvalue downwards. This is seen in table 1 by comparing the second and third columns. Calculations were performed in the half-contracted case in which the only (SS|SS) integrals included were for the contracted function. The effect on the highest positron eigenvalue was negligible, supporting the hypothesis that the core contracted functions do not affect the highest positron states. The issue of contraction of the core does not therefore seem to address the problem that for PbO there were eigenvalues which were above $-2mc^2$ by hundreds of hartrees when the core (SS|SS) integrals were added.

In itself, the occurrence of positron states above $-2mc^2$ is not unphysical. It indicates bound positrons, just as electron states below zero energy indicate bound electrons. That atoms or molecules should be able to bind positrons should not be surprising, considering their ability to bind protons. In calculations on the F^- ion, states at about $0.1 E_h$ above $-2mc^2$ were observed – a much more realistic value for a positron affinity. A similar observation was made by Visscher et al. [5] for EuO_6^{9-} , where, as for F^- , the long-range potential is attractive for positrons. The size of these “positron affinities” for PbO, $400 E_h$, is much too great to be a physical effect.

States significantly above $-2mc^2$ have also been noted by Visscher et al. [5] when the Aitken extrapolation procedure was used in the SCF process to accelerate convergence, but at convergence the states were no longer above $-2mc^2$. Several different methods for converging the PbO calculations, including the (SS|SS) integrals for the Pb 1s, 2s and 2p orbitals only, were tried: level shifting, DIIS [6] extrapolation on the off-diagonal blocks of the Fock matrix or on the differences in the coefficients between iterations, damping on the density matrix or

on the coefficients, and various combinations of these. None had any effect on the intruder state.

Because of the resources needed for complete calculations on PbO, further tests were carried out on SnO. Three different calculations were performed. In the first, the (LL|SS) and (SS|SS) integrals involving the small-component valence basis functions were omitted, in the second only the (SS|SS) integrals over the valence basis functions were omitted, and in the third all integrals were included. In the first calculation, the highest positron eigenvalue was at $153.56 E_h$ above $-2mc^2$, and was not the only one above $-2mc^2$. The two highest positron states had large coefficients from the Sn core s functions, and were the highest positron states composed of these functions. Similarly, the PbO intruder had large coefficients of the Pb core s functions, and was the highest positron state composed of these functions. In the second calculation on SnO, which used the vectors from the first calculation as a starting guess, the highest positron state was $0.106 E_h$ below $-2mc^2$, and it had only small contributions from the Sn core s functions. In the third it rose slightly, to $0.081 E_h$ below $-2mc^2$, in accordance with the behaviour expected from the arguments presented above.

The evidence to this point suggests that the complete omission of a class of integrals – such as (SS|SS) – does not produce intruder states, but that addition of only some of the integrals of a given class may do so. In the calculations on PbO, the first stage included the (LL|LL) and (LL|SS) integrals. The addition of the (SS|SS) integrals for the Pb $n=1$ and 2 shells produced upward shifts in elements of the Fock matrix in the atomic spinor basis of the order of $10 E_h$, a not unreasonable shift. This shift was magnified to $90 E_h$ for the highest core s-like positron state in the molecular spinor basis due to the large coefficients in the trial vectors, which were taken from the first stage of the calculation. Clearly, the (SS|SS) integrals which were added make a significant contribution to the Fock matrix and cannot be omitted at any stage of the calculation. The absence of these integrals in the first stage of the calculation produces a distortion in the positron eigenvectors which, when the integrals are put back in, gives rise to the intruder states. The same appears to be true of the valence (LL|SS) integrals in the calculations on SnO. While the omission of the valence (SS|SS)

integrals for SnO appears to have had very little effect on the positron spectrum, it remains to be seen whether this will be true for heavier systems such as PbO. It should be pointed out that for PbO, only some of the core (SS|SS) integrals were put back into the calculation. If the remaining core (SS|SS) integrals were included, the intruder could disappear as it did for SnO. It is clear also that the procedure in which the classes of integrals, (LL|LL), (LL|SS) and (SS|SS), are added in stages has some role to play in the appearance of intruder states. A better, but more time-consuming, procedure would be to use all the integrals and build up the electron occupation from the core.

The relation of the appearance of intruder states to the large size of some of the coefficients in the molecular spinor expansion re-opens the question of core contraction. It may be that the inflexibility of the general contraction in the core does not permit a sufficiently good description of the corresponding positron states to avoid the appearance of intruders; it may be that all of the core integrals are necessary to ensure that the contracted functions do give a good description of the positron states, or it may be simply that certain classes of integrals cannot be omitted regardless of the nature of the contraction. Addition of extra functions for the small component in order to give it a better description is to be avoided for several reasons. The first is that the additional functions will add significantly to the cost of any calculations – not a small consideration, given the large number of integrals required. The second is that generally contracted core functions taken from atomic calculation should provide a good description of the molecular core, and thus any additional functions will only go into the description of the positron states, which are not of interest for most molecular applications. The third is the matching of functions for small and large components and their one-to-one correspondence with electron and positron states, required by physical considerations [7].

An alternative to the current general contraction scheme, which uses the atomic SCF functions, is to transform the core basis functions to a form in which they are readily localized – “nodeless” functions. While the same space would be covered by these functions, the effect of inclusion of a small subset of the (SS|SS) integrals from these functions in cal-

culations such as were done for PbO should be markedly different. The inner tail of the core functions is the part from which the largest (SS|SS) integral contribution comes: in the atomic contraction scheme, each function has its own inner tail, whereas in the radially localized contraction scheme, there is only one function for the inner tail. Thus, adding (SS|SS) integrals for only a few core functions in the atomic scheme creates a very uneven distribution of the inner tail contribution, but in the radially localized scheme, most of the inner tail contribution is obtained, and it is more evenly distributed.

To test this hypothesis, radially localized functions (RLFs) were generated from the atomic functions in a Gaussian basis as follows. Each RLF for a given n quantum number was expressed as a linear combination of the atomic function and the RLFs with lower n value:

$$\phi_n^{\text{loc}} = \phi_n - \sum_{k=1}^{n-1} c_{nk} \phi_k^{\text{loc}}. \quad (4)$$

Each function is expressed as a linear combination of Gaussian functions g_μ ,

$$\phi_k^{\text{loc}} = \sum_{\mu=1}^N b_{k\mu} g_\mu, \quad \phi_k = \sum_{\mu=1}^N a_{k\mu} g_\mu, \quad (5)$$

so that the RLF can be written

$$\phi_n^{\text{loc}} = \sum_{\mu=1}^N \left(a_{n\mu} - \sum_{k=1}^{n-1} c_{nk} b_{k\mu} \right) g_\mu. \quad (6)$$

A convenient way of performing the radial localization is to minimize the coefficients of the Gaussian expansion of the RLF over some range of exponents. We choose the function to be minimized as the weighted sum of the squared coefficients,

$$F = \sum_{\mu=1}^{n_c} w_\mu \left(a_{n\mu} - \sum_{k=1}^{n-1} c_{nk} b_{k\mu} \right)^2, \quad (7)$$

with weights $w_\mu = \sqrt{\zeta_\mu}$, where ζ_μ is the exponent of Gaussian μ , and the cutoff value for the sum, n_c , is chosen to correspond to the $(n-1)$ th radial node. Both the atomic functions and the radially localized functions have been used in a series of calculations on PbO at $r = 3.6 a_0$. The first stage of the calculations included only the (LL|LL) and (LL|SS) integrals. At each succeeding stage, (SS|SS) integrals were added for the next highest n quantum number on Pb,

Table 3

Effect of contraction scheme on the highest positron eigenvalue and the total energy and energy change as successive shells of (SS|SS) integrals are added to calculations on PbO at $3.6 a_0$. Eigenvalue is given relative to $-2mc^2$. First row has results without (SS|SS) integrals. All energies are given in E_h .

(SS SS) integrals added	Atomic SCF contraction			Radially localized contraction		
	eigenvalue	E_{tot}	ΔE_{tot}	eigenvalue	E_{tot}	ΔE_{tot}
	-0.1583	-20989.59304		-0.1583	-20989.59304	
$n=1$	-0.1579	-20989.02265	+0.57039	-0.1583	-20988.68970	+0.90334
$n=2$	+128.06	-20986.72719	+2.29546	-0.1578	-20985.36697	+3.32273
$n=3$	+468.55	-20984.96186	+1.76533	-0.1576	-20984.39280	+0.97417
$n=4$	+619.94	-20984.85034	+0.11152	-0.1569	-20985.22919	-0.83639
$n=5$	-0.1580	-20986.74701	-1.89037	-0.1580	-20986.74071	-1.51152

starting with Pb $n=1$, and adding the O $n=1$ and 2 with the Pb $n=4$ and 5 integrals. The results are presented in table 3, labelled with the Pb n quantum number. Three features emerge from this study, confirming the hypothesis made above. The first is that there are *no* intruder states in the series of calculations with the RLFs. The highest positron eigenvalue displays a small upward shift as the (SS|SS) integrals are successively added. The second is that a larger energy contribution is obtained from the lower n (SS|SS) integrals using RLFs than using the atomic functions. Both of these indicate that the contributions for all the core functions are being added in order of importance in the RLF series of calculations. The third is that at $n=5$, the two calculations give the same results, as expected, and no intruder states are in evidence.

The conclusion of this investigation is that the appearance of the intruder states was related not to general contraction per se, or to the SCF convergence method, but to the particular general contraction scheme used. To ensure that they do not appear, either all of the core (SS|SS) integrals have to be included in the calculation, or if this is not feasible, a radially localized contraction scheme should be employed to ensure a more even distribution of the (SS|SS) contributions to the Fock matrix. The cal-

culations on SnO indicate that it is possible to perform meaningful calculations which omit the valence (SS|SS) integrals. However, care must always be exercised in the omission of classes of integrals, and there may be cases in which it is not possible to omit subsets of integrals involving the small component. This would restrict the range of problems which could be tackled with the DHF method using conventional SCF procedures and current storage availability.

The author was supported by NASA grant No. NCC2-552, and would like to thank Dr. Winifred Huo and Dr. Peter Taylor for helpful discussions.

References

- [1] K.G. Dyall, P.R. Taylor, K. Fægri Jr. and H. Partridge, *J. Chem. Phys.* 95 (1991) 2583.
- [2] K.G. Dyall, *J. Chem. Phys.* 96 (1992) 1210.
- [3] P. Chaix and D. Iracene, *J. Phys. B* 22 (1989) 3791.
- [4] K. Fægri Jr., Technical note, Department of Chemistry, University of Oslo.
- [5] L. Visscher, P.J.C. Aerts, O. Visser and W.C. Nieuwpoort, *Intern. J. Quantum Chem. Symp.* 25 (1991) 131.
- [6] P. Pulay, *Chem. Phys. Letters* 73 (1980) 393.
- [7] I.P. Grant and H.M. Quiney, *Advan. At. Mol. Phys.* 23 (37) 1988.

The ${}^2\Sigma^+ - {}^2\Pi$ separation in KO

Charles W. Bauschlicher Jr. and Harry Partridge
NASA Ames Research Center
Moffett Field, CA 94035

Kenneth G. Dyall
ELORET Institute†
Palo Alto, CA 94303

Abstract

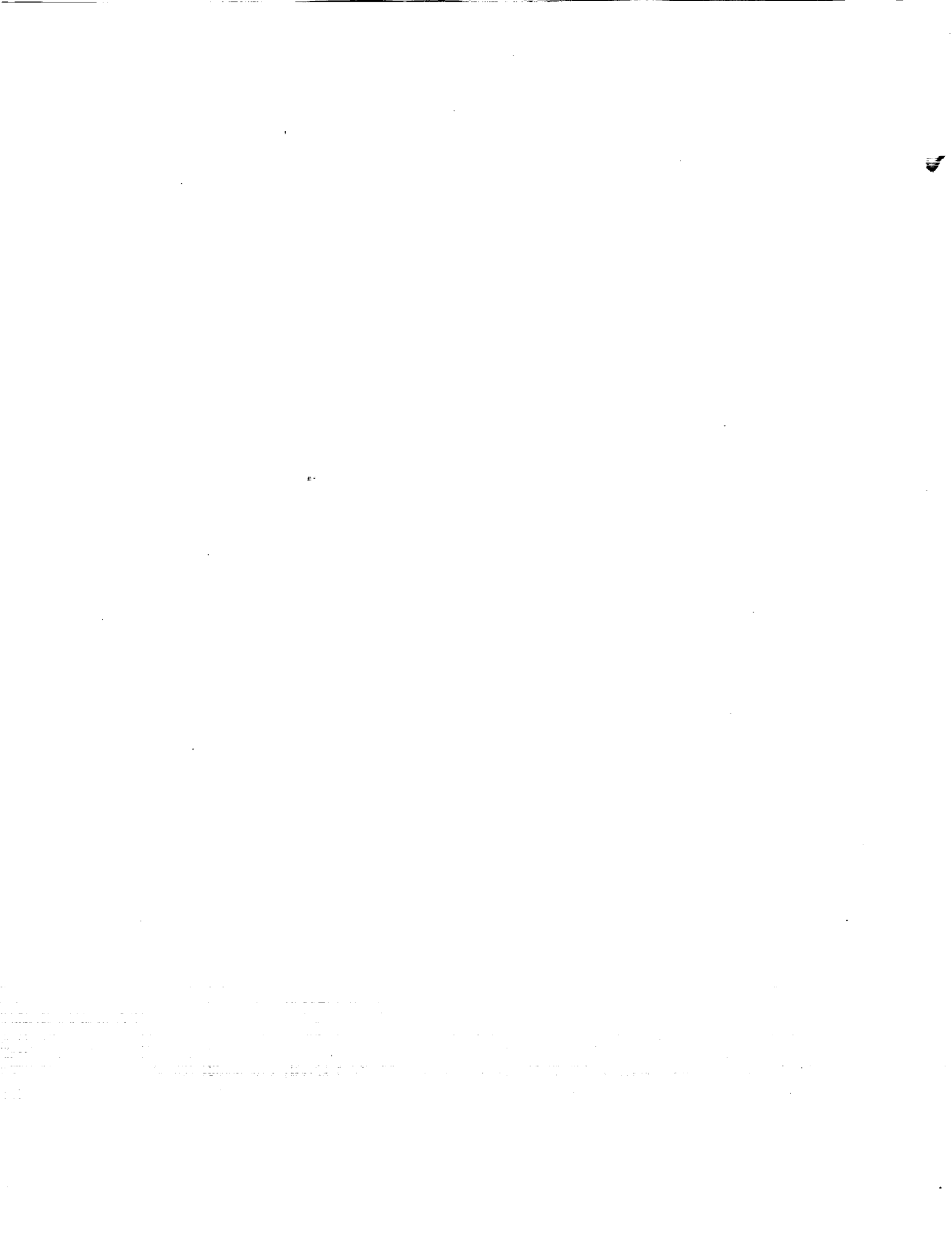
The ${}^2\Sigma^+ - {}^2\Pi$ separation in KO is investigated using large basis sets and high levels of correlation treatment. Relativistic effects are included at the Dirac-Fock level and reduce the separation only slightly. The basis set superposition error is considered in detail. On the basis of these calculations, our best estimate places the ${}^2\Pi_{3/2}$ state about 200 cm^{-1} above the ground ${}^2\Sigma^+$ state in agreement with our previous estimate.

I. Introduction

In 1986 we computed the ${}^2\Sigma^+ - {}^2\Pi$ separation in KO to be 238 cm^{-1} with the ${}^2\Sigma^+$ state being the lower of the two [1]. This separation was computed at the singles and doubles configuration interaction (SDCI) level using a large Slater basis set. While not definitive, the separation was thought to be accurate because of the small difference between the SDCI and self-consistent-field (SCF) values. However, when 15 electrons are correlated, an SDCI treatment can underestimate the differential correlation effects. Approaches such as the modified coupled-pair functional (MCPF) method [2], or the coupled cluster singles and doubles method with a perturbational estimate of the triple excitations [3] [CCSD(T)], account for the effect of higher than double excitations and can therefore yield superior results to the SDCI approach.

Experimentally, the ground state has not been determined and there is conflicting evidence. The failure to observe an electron spin resonance (ESR) spectrum [4] is consistent with a ${}^2\Pi$ ground state, while the magnetic deflection experiments [5] suggest a ${}^2\Sigma^+$ ground state. Photoelectron detachment experiments [6] on KO^-

† Mailing address: NASA Ames Research Center, Moffett Field, CA 94035-1000



might offer a mechanism to directly observe both states, and hence determine the ground state and the separation; such experiments [6] have recently been performed for NaO^- and preliminary results suggest that they are possible for all of the alkali oxides systems. In addition, microwave experiments [7] have recently been performed on NaO and, with a pure-precession hypothesis, an estimate of the ${}^2\Sigma^+ - {}^2\Pi$ separation was obtained. An analogous experiment should be possible for KO .

Given the recent experimental activity on the alkali oxides, it seems timely to reinvestigate the ${}^2\Sigma^+ - {}^2\Pi$ separation in KO at higher levels of theory. We consider the effect of one-particle basis set and basis set superposition error (BSSE) in more detail than in our previous work. In addition, the separation between the ${}^2\Sigma^+$ and ${}^2\Pi$ states is small enough that relativistic effects could affect the ordering of the states. These were not included in the previous work and are addressed here.

II. Methods

Two basis sets are used in this work. The small oxygen basis set is the $(13s\ 9p\ 6d\ 4f)/[5s\ 5p\ (2+1)d\ 1f]$ atomic natural orbital [8] (ANO) set [9] determined from the average natural orbitals of O and O^- . (The notation $n+m$ indicates n ANO orbitals are employed and m primitive functions are uncontracted). In the large oxygen basis set only two s and one p ANOs are used. The outer five s and five p primitives and the d and f polarization functions are uncontracted. This is augmented with two uncontracted g functions and a diffuse s function with an orbital exponent of 0.076666. Thus the final basis set is of the form $(14s\ 9p\ 6d\ 4f\ 2g)/[(2+6)s\ (1+5)p\ 6d\ 4f\ 2g]$.

The small K basis is derived from the $(24s\ 15p)$ basis [10] augmented with an s function optimized for K^- and three p functions optimized for the 2P state of K . The s and p basis sets are contracted to $(3+6)$ and $(2+7)$, respectively, where the three s and two p contraction coefficients are taken from the SCF wave function. The basis is further augmented with six even-tempered ($\alpha_n = 2.5^n \alpha_0$ for $n=0, k$) d functions with $\alpha_0 = 0.0455$ and four even-tempered f functions with $\alpha_0 = 0.12949$. The small K basis set is of the form $(25s\ 18p\ 6d\ 4f)/[(3+6)s\ (2+7)p\ 6d\ 4f]$. In the large K basis set, the s and p functions are contracted $(2+12)$ and $(2+9)$ and two g functions ($\alpha = 0.768$ and 0.307) are added, thus yielding a basis set of the form $(25s\ 18p\ 6d\ 4f\ 2g)/[(2+12)s\ (2+9)p\ 6d\ 4f\ 2g]$. Only the pure spherical harmonic components of the basis functions are used.



The orbitals are optimized using the SCF approach. We have treated the ${}^2\Pi$ state using symmetry and equivalence restrictions (i.e., a $\pi_x^{1.5}\pi_y^{1.5}$ occupation) or by using a symmetry broken solution (i.e., a $\pi_x^2\pi_y^1$ occupation). Electron correlation is added using the MCPF or CCSD(T) approaches. Fifteen electrons are correlated, corresponding to the O 2s and 2p and the K 3s, 3p, and 4s electrons.

Relativistic effects are estimated as the difference between the SCF and Dirac-Fock (DF) results. Because correlation was not included, it was possible to reduce the basis set size without affecting the accuracy of the results. The full *s* and *p* primitive basis sets for K and O were contracted to $[(3 + 6)s (2 + 7)p]$ and $[(2 + 3)s (1 + 4)p]$ using the orbitals from the SCF wave functions for K^+ and O^- . For polarization the 6*d* set and the outer three of the 4*f* functions on K were used, and on O the outer 3 primitive *d* functions and the *f* function with the largest coefficient from the ANO polarization set were used. The SCF ${}^2\Sigma^+ - {}^2\Pi$ separation in this basis set was identical to that found using the small ANO set.

The SCF/MCPF calculations were performed using the SEWARD [11]-SWEDEN [12] program system. The CCSD(T) calculations were performed using the program developed by Scuseria [13]. The atomic DF calculations were performed using GRASP [14] while the molecular calculations were performed using the code developed by Dyll [15]. All calculation were performed on the NASA Ames Central Computer Facility CRAY Y-MP or Computational Chemistry Branch IBM RISC System/6000 computers.

III. Results and Discussion

The separation at the SCF level is only slightly larger than in our previous work [1], with the big basis set result essentially reaching our previous estimate of 250 cm^{-1} for the numerical Hartree-Fock separation. The SDCI separation in the small basis set is only 6 cm^{-1} smaller than that reported in our previous study. With a symmetry broken SCF solution, the ${}^2\Pi$ state is predicted to be below the ${}^2\Sigma^+$ state. When correlation is added at the SDCI level, the ${}^2\Sigma^+$ state is predicted to be lower. However, the SDCI based on the symmetry broken SCF orbitals yields a significantly smaller separation. This suggests that the SDCI approach is unable to overcome the bias in the SCF wave function. At the MCPF level, the effect of symmetry breaking is smaller, as expected, since the MCPF approach includes the effect of higher excitations. At this level, the symmetry broken solution actually



leads to a larger separation than using the SCF with symmetry and equivalence restrictions. Both MCPF separations are about 100 cm^{-1} smaller than the SDCl result with symmetry and equivalence restrictions. The CCSD separation is the same as the MCPF. The effect of triples is to further increase the separation by 47 cm^{-1} , which is almost an order of magnitude smaller than the difference between the SCF and CCSD (368 cm^{-1}). This strongly suggests that even higher levels of theory will not significantly increase the correlation contribution to the separation. Expanding the basis set results in a small increase in both SCF and MCPF separations.

In Table II we report the BSSE at the MCPF level. We compute the BSSE for K^+ with the O basis set, $\text{K}^+(\text{O})$, and O^- with the K basis set, because both states of the molecule at r_e are best described as K^+O^- . K^+ is a closed shell; therefore the calculation of the BSSE is straightforward, and we consider $\text{K}^+(\text{O})$ at the two relevant internuclear separations. The $2p^5$ occupation of O^- is oriented $2p\sigma^2 2p\pi^3$ and $2p\sigma^1 2p\pi^4$ for the $^2\Pi$ and $^2\Sigma^+$ states, respectively. As shown in previous work [16], the BSSE can differ significantly for the two occupations. Therefore we use the BSSE for the $2p\sigma^2 2p\pi^3$ occupation to correct the $^2\Pi$ state and the BSSE for the $2p\sigma^1 2p\pi^4$ occupation to correct the $^2\Sigma^+$ state.

For K^+ the BSSE is small for both basis sets. It is slightly larger for the $^2\Sigma^+$ state than the $^2\Pi$ state because of the shorter bond length. In contrast, the O^- BSSE is much larger for the smaller basis set. In spite of the longer bond length, the $\text{O}^-(\text{K})$ BSSE is larger for the $^2\Pi$ state, because a pair of oxygen $2p\sigma$ electrons points at the ghost basis set compared with only one electron in the $^2\Sigma^+$ state. For both basis sets the total BSSE is very similar for the $^2\Sigma^+$ and $^2\Pi$ states and therefore does not have an important differential effect on the separation. Given the small total BSSE for the big basis set, this conclusion seems definitive in spite of any uncertainties in how to best compute the BSSE.

One effect not considered to this point is relativity. The spin-orbit splitting in the O^- ion was calculated to be 193 cm^{-1} at the Dirac-Coulomb level. Inclusion of the Breit interaction decreased the splitting to 170 cm^{-1} . This value is expected to be accurate as an analogous treatment of O agrees with experiment to within 2 cm^{-1} . Because the bonding in KO is best described as K^+O^- , this splitting in O^- can be used in a simple first-order model [17] to estimate the splitting in KO. On this basis, the $^2\Sigma_{1/2}^+$ state is unshifted from its nonrelativistic position, the $^2\Pi_{1/2}$



1. The first part of the document discusses the importance of maintaining accurate records of all transactions and activities. This is essential for ensuring transparency and accountability in the organization's operations. The second part outlines the specific procedures and protocols that must be followed to ensure compliance with all relevant laws and regulations. Finally, the document concludes with a strong emphasis on the need for ongoing monitoring and evaluation to ensure that all standards are consistently met and any issues are promptly addressed.

state is shifted up by 57 cm^{-1} and the ${}^2\Pi_{3/2}$ state is shifted down by 57 cm^{-1} .

Mixing of K $4s$ character from covalent contributions to the wave functions and spin-orbit mixing of the ${}^2\Pi_{1/2}$ and ${}^2\Sigma_{1/2}^+$ states could invalidate the first-order model. Therefore we study the ${}^2\Pi_{3/2}$ and ${}^2\Sigma_{1/2}^+$ states at the Dirac-Fock level. On the basis of the nonrelativistic calculations we use a bond length of $4.4 a_0$ for the ${}^2\Pi_{3/2}$ state and $4.13 a_0$ for the ${}^2\Sigma_{1/2}^+$ state. At this level, the ${}^2\Pi_{3/2}$ state is lowered by 36 cm^{-1} and the ${}^2\Sigma_{1/2}^+$ state is lowered by 24 cm^{-1} , relative to the nonrelativistic states. Thus the differential effect of relativity on the state separation is only 12 cm^{-1} , or about $1/5$ of the estimate derived from O^- . Clearly, however, the differential effect of relativity is sufficiently small that it will not reverse the order of the states computed at the nonrelativistic level.

Our best separation is obtained by correcting the CCSD(T) separation for: 1) MCPF basis set improvement ($+36 \text{ cm}^{-1}$), 2) BSSE ($+8 \text{ cm}^{-1}$) and 3) relativistic effects (-12 cm^{-1}). This yields a separation of 214 cm^{-1} , with the ${}^2\Sigma^+$ state being lower. This is very similar to our previous result [1]. While it is difficult to be definitive for a separation this small, the calculations strongly suggest that the ground state is ${}^2\Sigma^+$. Because improving the basis set increases the separation, as does including higher levels of correlation treatment, and relativistic effects are very small, it is difficult to imagine what effect would reverse the order of these two states.

IV. Conclusions

The separation at our highest level of theory, the CCSD(T) approach, is 182 cm^{-1} . Including the correction for basis set incompleteness from the MCPF level increases the separation to 218 cm^{-1} , which is very similar to our previous result [1]. The differential effect of BSSE is 8 cm^{-1} , increasing the separation. Relativistic effects reduce the separation by only 12 cm^{-1} . Thus we conclude that the ground state is ${}^2\Sigma^+$.

References

1. S. R. Langhoff, C. W. Bauschlicher, and H. Partridge, *J. Chem. Phys.* 84 (1986) 4474. S. R. Langhoff, C. W. Bauschlicher, and H. Partridge, in "Comparison of Ab Initio Quantum Chemistry with Experiment" R. J. Bartlett, ed., D. Reidel Publishing Co. Boston (1985).
2. D. P. Chong and S. R. Langhoff, *J. Chem. Phys.* 84 (1986) 5606. See also R. Ahlrichs, P. Scharf, and C. Ehrhardt, *J. Chem. Phys.* 82 (1985) 890.
3. R. J. Bartlett, *Annu. Rev. Phys. Chem.* 32 (1981) 359; K. Raghavachari, G. W. Trucks, J. A. Pople, and M. Head-Gordon, *Chem. Phys. Lett.* 157 (1989) 479.
4. D. M. Lindsay, D. R. Herschbach, and A. L. Kwiram, *J. Chem. Phys.* 60 (1974) 315.
5. R. R. Herm and D. R. Herschbach, *J. Chem. Phys.* 52 (1970) 5783.
6. K. H. Bowen, personal communication.
7. C. Yamada, M. Fujitake, and E. Hirota, *J. Chem. Phys.* 90 (1989) 3033.
8. J. Almlöf and P. R. Taylor, *J. Chem. Phys.* 86 (1987) 4070.
9. C. W. Bauschlicher, H. Partridge, and S. R. Langhoff, *Chem. Phys.* 148 (1990) 57.
10. H. Partridge, *J. Chem. Phys.* 90 (1989) 1043.
11. R. Lindh, U. Ryu, and B. Liu, *J. Chem. Phys.* 95 (1991) 5889.
12. SWEDEN is an electronic structure program written by J. Almlöf, C. W. Bauschlicher, M. R. A. Blomberg, D. P. Chong, A. Heiberg, S. R. Langhoff, P.-Å. Malmqvist, A. P. Rendell, B. O. Ross, P. E. M. Siegbahn, and P. R. Taylor.
13. G. E. Scuseria, *Chem. Phys. Lett.* 176 (1991) 27.
14. K. G. Dyall, I. P. Grant, C. T. Johnson, F. A. Parpia, and E. P. Plummer, *Computer Phys. Commun.* 55 (1989) 425.
15. Open-shell DF code: K. G. Dyall, to be published, follows same methods as Closed-shell code, K. G. Dyall, K. Fægri, Jr., P. R. Taylor, and H. Partridge, *J. Chem. Phys.* 95 (1991) 2583.
16. H. Partridge, C. W. Bauschlicher, and S. R. Langhoff, *Theor. Chim. Acta.* 77 (1990) 323.
17. Lefebvre-Brion, H.; Field, R. W., *Perturbations in the Spectra of Diatomic*



Molecules (Academic Press, Inc.; Orlando; 1986.)



Table II. Summary of the BSSE at the MCPF level.

	BSSE(cm ⁻¹)
Small basis set	
² Σ ⁺	
K ⁺ (O) at r=4.13	32.1
O ⁻ (K) at r=4.13	348.4
Total	380.5
² Π	
K ⁺ (O) at r=4.40	20.9
O ⁻ (K) at r=4.40	364.5
Total	385.4
Big basis set	
² Σ ⁺	
K ⁺ (O) at r=4.13	32.5
O ⁻ (K) at r=4.13	88.5
Total	121.0
² Π	
K ⁺ (O) at r=4.40	25.8
O ⁻ (K) at r=4.40	103.4
Total	129.2



**All-electron molecular Dirac-Hartree-Fock calculations:
properties of the Group IV monoxides GeO, SnO and PbO.**

Kenneth G. Dyall *,
Eloret Institute, 3788 Fabian Way, Palo Alto,
California 94303, U.S.A.

Abstract

Dirac-Hartree-Fock calculations have been carried out on the ground states of the group IV monoxides GeO, SnO and PbO. Geometries, dipole moments and infrared data are presented. For comparison, nonrelativistic, first-order perturbation and relativistic effective core potential calculations have also been carried out. Where appropriate the results are compared with the experimental data and previous calculations. Spin-orbit effects are of great importance for PbO, where first-order perturbation theory including only the mass-velocity and Darwin terms is inadequate to predict the relativistic corrections to the properties. The relativistic effective core potential results show a larger deviation from the all-electron values than for the hydrides, and confirm the conclusions drawn on the basis of the hydride calculations.

* Mailing address: NASA Ames Research Center, MS RTC 230-3, Moffett Field,
CA 94035-1000, U.S.A.



I. INTRODUCTION

Relativistic effects are known to be important in the chemistry of the heavy elements, but how important is an issue which can only be decided on the basis of accurate calculations. The demands of calculations on molecules containing heavy elements including relativistic effects are such that until recently, various approximate methods had to be employed to reduce the size of the calculations. All such methods are based in some way on the Dirac equation, which is in turn an approximation to equations derived from quantum electrodynamics [1].

The most common approximation is the use of a relativistic effective core potential (RECP) [2,3] in which the Dirac equation itself or an approximation to it such as the Cowan-Griffin equation [4] is used to generate valence pseudo-orbitals from which the effective potential is constructed. Usually, the spin-dependent terms are averaged out to give an RECP which can be used with standard nonrelativistic codes. Several sets of RECPs have been published [5-8,9].

Some other approaches, which do not depend on the frozen-core approximation as do the RECPs, are first-order perturbation theory (PT) with the spin-free terms — the mass-velocity and Darwin (MVD) terms — in the perturbation Hamiltonian [4,10], and the spin-free no-pair method of Hess *et al.* [11,12]. These are based on a transformation of the Dirac equation to eliminate the small component to a given order and truncation of the resultant expression to obtain a spin-free Hamiltonian. The method of Hess *et al.* provides a Hamiltonian which can be used in variational calculations, whereas the MVD operator is strictly a perturbation operator.

The past few years has seen the development of some all-electron Dirac-Hartree-Fock (DHF) codes [13-15]. Methods for inclusion of electron correlation based on these codes are only now being developed [16]. Although correlation effects are important in obtaining quantitative predictions of molecular properties, it is important to calibrate the various approximations to the Dirac equation at the self-consistent field (SCF) level, because if the approximate methods are inaccurate at

the SCF level, they can only provide correlated results in agreement with experiment by accident.

This paper is the third of a series examining relativistic effects on properties of small molecules containing Group IV elements, and providing calibration of RECP and PT methods. The first and second papers [17,18], hereafter referred to as I and II, were concerned with the hydrides. Despite the shortness of the bond lengths, hydrogen offers only a small perturbation to the central atom. Introducing a heavier atom should give a better test of the quality of the approximate methods. In this paper the properties of the monoxides of Ge, Sn and Pb are examined using nonrelativistic (NR) SCF, PT including only the MVD terms, RECPs, and the DHF method.

The monoxides are well-known experimentally [19]. Previous calculations have been performed on PbO by Basch *et al.* [20] at the SCF and multi-configuration self-consistent field (MCSCF) levels of theory using RECPs, by Schwenzner *et al.* [21] at the NR SCF level, by Datta *et al.* [22] at the SCF level using both relativistic and nonrelativistic ECPs, and by Balasubramanian and Pitzer [23] at the singles and doubles configuration interaction (SDCI) level with an RECP for lead and including spin-orbit interaction at the CI stage. Balasubramanian and Pitzer have performed similar calculations SnO [24]. Igel-Mann *et al.* [25] have studied SnO and other molecules extensively, at the SCF, complete active space self-consistent field (CASSCF) and SDCI levels using RECPs with a core polarization potential and several basis sets. Bouteiller *et al.* [8] have performed calculations on GeO (among other molecules) at the SCF level, both all-electron and with an ECP. Comparisons are made with these calculations where appropriate.

II. COMPUTATIONAL DETAILS

The primitive basis sets used for the group IV elements were the same as used in I and II. The exponents were energy-optimized in nonrelativistic SCF calculations and are of approximately valence double-zeta quality. The *d* basis set was



supplemented with 2 extra functions to describe valence polarization. The primitive basis set for oxygen was the van Duijneveldt [26] 11s6p basis supplemented with a diffuse *s* and *p* function to help describe the negative-ion character in the molecules, and 2 *d* polarization functions taken from Dunning's [27] pVTZ basis. Contraction coefficients for all basis sets were determined from atomic SCF calculations using a general contraction scheme. The relativistic contraction coefficients were obtained from an adaption of GRASP [28], as described in I. For the Group IV elements, all functions up to the $(n - 1)d$ shell were kept in the core, and the outermost three *s*, *p* and *d* primitive functions were uncontracted to form the valence basis. The O basis was contracted to 5s4p2d, with three uncontracted *s* and *p* functions in the valence basis, and the inner tails of the 2s and 2p functions in the core.

Four sets of RECPs were used for Ge, Sn and Pb: those of Hay and Wadt [5] (hereafter referred to as HW), those of Stevens, Krauss, Basch and Jasien [6] (hereafter referred to as SKBJ), and both the full-core and the semi-core potentials of Ref. 7 (hereafter referred to as CER and CER+*d* respectively). Only the spin-averaged potentials (averaged relativistic effective potentials, AREPs) from ref. 7 are used in this work. Both the valence *sp* basis sets from the all-electron calculations and the *sp* basis sets supplied with the RECPs, contracted to 3s3p, were used in the RECP calculations, supplemented by the valence *d* functions from the all-electron basis set. The *d* orbital supplied with the CER+*d* basis was left fully contracted.

The equilibrium geometry of the molecules was determined from a quartic fit to 5 or 6 points around r_e . The energy at the predicted r_e was added to the fit to determine the force constants. A quartic fit to the dipole moments was also used to determine the dipole derivatives at r_e . The program INTDER [29] was used to obtain the harmonic frequencies and infrared intensities. The isotopes used for the frequencies were ^{16}O , ^{74}Ge , ^{120}Sn and ^{208}Pb . All properties are reported at the predicted r_e value for each method. The value of the speed of light in atomic units was taken to be 137.03604.

The MOLECULE/SWEDEN [30] package was used to obtain the NR SCF,



PT and RECP results. DHF results were obtained with the program described previously [15,17]. To limit the size of the DHF calculations, it has been found useful to discard all of the integrals involving the small component valence basis functions [17,31]. This has a negligible effect on the properties even for Pb compounds, because the terms omitted contribute the energy only at $\mathcal{O}(\alpha^4)$. In the present calculations these (SS|SS) integrals were discarded for PbO. All calculations were performed on the Computational Chemistry Branch Convex C-210 and the Central Computing Facility CRAY Y-MP/864 computers at NASA Ames Research Center.

III. RESULTS AND DISCUSSION

The calculated bond lengths r_e are presented in Table I, along with the experimental values [19], and the relativistic corrections to the bond lengths $\Delta^{rel}r_e$ predicted by the PT and DHF calculations. The dipole moment data are presented in Table II, and the harmonic frequencies and infrared (IR) intensities in Table III. The first part of the discussion deals with the all-electron data and the properties of the molecules in general, in the second part the RECP data are discussed and compared with the all-electron data, and in the third, comparisons are made with other calculations.

A. All-electron results.

An understanding of the differences in properties of the group IV monoxides is aided by consideration of the relative energies of the atomic orbitals. The orbital energies for Ge, Sn, Pb and O obtained from configuration average SCF calculations are given in Table IV. The O 2s orbital is close to the *d* orbital on the metal, and the metal *s* orbital is close to the O 2*p* orbital. It is therefore expected that the O 2s orbital will not participate much in the bonding. The table also shows that Sn has the least bound valence orbitals when relativistic effects are included (the 6*p*_{3/2} is unoccupied in the ground configuration of Pb): experimentally, Sn has the smallest ionization potential (IP) in the group. Sn may thus be expected to give the most ionic oxide. This conclusion would not be borne out by nonrelativistic



calculations, for which the IP decreases monotonically down the group.

The relativistic bond length corrections are smaller than those of the hydrides. Most of the bond length contraction resulting from the spin-free terms in the relativistic Hamiltonian is cancelled by the spin-orbit interaction, which causes a partial promotion of σ electrons into π orbitals that are usually of antibonding character. Comparison of the DHF bond lengths with experiment shows a uniform underestimate of 0.03\AA , partly due to basis set effects and partly to electron correlation.

The dipole moments mostly show very little change from relativistic effects. There is a small increase for GeO and SnO, and the spin-free terms give a small decrease for PbO. The dipole moment of PbO is reduced significantly at the DHF level, because of significant changes in the valence molecular spinors (MSs) from their nonrelativistic counterparts. PT is unable to describe these changes, and thus does not give an accurate value for $\overline{\mu_e}$. The DHF atomic charges obtained by dividing μ_e by r_e show SnO more ionic than GeO by $0.07e$, and PbO less ionic than SnO by $0.01e$. Without spin-orbit interaction, PbO is more ionic than SnO by $0.02e$. It should be noted that the dipole moments reported here include effects from both geometric and electronic structural changes due to relativity. If the dipole moments at a fixed geometry are considered, the changes are larger. For PbO at $3.6a_0$, for instance, PT gives a relativistic correction of 0.27 D , compared to the DHF correction of -0.13 D . The spin-orbit effect at $3.6a_0$ is then -0.40 D , rather than the -0.20 D obtained by comparing results at the respective r_e values.

It is for the IR harmonic frequencies and intensities that the effect of spin-orbit interaction is most dramatic, resulting in a 10% reduction in the frequency for PbO, and more than halving the intensity. The changes in the valence MSs bring about a large decrease in the dipole derivative. PT obtains only 7% of the frequency reduction, and predicts an increased intensity. The frequency reduction is smaller for SnO but PT still obtains only a fraction of it, whereas for GeO spin-orbit effects are small enough that PT gives a satisfactory result. For the intensities of GeO and SnO, spin-orbit interaction apparently has no effect.

It is clear that spin-orbit interaction has a strong influence on the properties of PbO and by inference on the bonding. The nature of the bonding in heavy p -block diatomic molecules is strongly influenced by spin-orbit interaction and must be discussed in terms of ω - ω coupling. Several authors have discussed aspects of the bonding for the p -block elements [32-34]; the discussion is presented and extended here. Both $p_{1/2}$ and $p_{3/2}$ atomic spinors may contribute to $\omega = 1/2$ molecular spinors. The form of these atomic spinors (with $m_j \equiv \omega = 1/2$) is

$$p_{1/2} = \frac{1}{\sqrt{3}} \begin{pmatrix} -p\sigma \\ \sqrt{2}p\pi \end{pmatrix}; \quad p_{3/2} = \frac{1}{\sqrt{3}} \begin{pmatrix} \sqrt{2}p\sigma \\ p\pi \end{pmatrix} \quad (1)$$

An $\omega = 1/2$ molecular spinor may be written

$$\begin{aligned} \psi_{1/2} &= c_1 p_{1/2}^A + c_2 p_{1/2}^B + c_3 p_{3/2}^A + c_4 p_{3/2}^B \\ &= \begin{pmatrix} p\sigma_A(\sqrt{2}c_3 - c_1) + p\sigma_B(\sqrt{2}c_4 - c_2) \\ p\pi_A(\sqrt{2}c_1 + c_3) + p\pi_B(\sqrt{2}c_2 + c_4) \end{pmatrix} \end{aligned} \quad (2)$$

The bonding character of the spinors will be determined by the coefficients.

For homonuclear diatomics, $c_1 = \pm c_2$ and $c_3 = \pm c_4$ for the u and g combinations, giving

$$\begin{aligned} \psi_{1/2g} &= \begin{pmatrix} p\sigma_g(\sqrt{2}c_3 - c_1) \\ p\pi_g(\sqrt{2}c_1 + c_3) \end{pmatrix} \\ \psi_{1/2u} &= \begin{pmatrix} p\sigma_u(\sqrt{2}c_3 - c_1) \\ p\pi_u(\sqrt{2}c_1 + c_3) \end{pmatrix} \end{aligned} \quad (3)$$

The molecular symmetry thus imposes on the spinors a mixture of bonding and antibonding character, which is determined by the ratio of the coefficients c_1 and c_3 . The λ - s coupling limit is obtained with $c_1 = \sqrt{2}c_3$ for a pure $\pi\beta$ spinor or $c_3 = -\sqrt{2}c_1$ for a pure $\sigma\alpha$ spinor. This requires a promotion from the $p_{1/2}$ to the $p_{3/2}$ atomic spinor, which for light elements is negligible, but for heavy elements can be considerable, resulting in weaker bonds. In Tl_2 for instance, the promotion cost is sufficient to render the lowest 0_g^+ state bound by only 0.01eV at the 2-configuration SCF level [33], and the ground state is the 0_u^- state from the configuration $(1/2_g)^1(1/2_u)^1$, bound by only 0.04eV.



For heteronuclear diatomics, the coefficients are not restricted by the g/u symmetry as they are for homonuclear diatomics, and hence the σ -bonding/ π -antibonding and σ -antibonding/ π -bonding combinations need not arise. The restrictions will instead be on the ratios of c_1 to c_2 and c_3 to c_4 , determined by the magnitude of the spin-orbit splitting of the p shell on each centre. For small spin-orbit splittings the λ - s coupling limit is obtained with coefficients as for the homonuclear case. In the extreme of large spin-orbit splitting on centre A, it is possible to obtain pure bonding spinors with $c_3 = c_2 = 0$:

$$\psi_{1/2} = \begin{pmatrix} -p\sigma_A + \sqrt{2}p\sigma_B \\ \sqrt{2}p\pi_A + p\pi_B \end{pmatrix}. \quad (4)$$

In this spinor, the σ component is skewed towards centre B and the π component towards centre A . This kind of combination of atomic spinors would be favoured in SCF energy optimization. The opposite skewing is obtained with $c_1 = c_4 = 0$, but is not favoured for large spin-orbit splitting on centre A due to the promotion cost.

The DHF Mulliken gross populations presented in Table V and the integrated spin densities presented in Table VI illustrate well the trend from small to large spin-orbit interaction. For GeO with small spin-orbit interaction, the $p_{1/2} : p_{3/2}$ ratios are close to the 1:2 ratio required for a σ orbital with α spin in the $12e_{1/2}$ and $14e_{1/2}$ spinors and 2:1 for a π orbital with β spin in the $13e_{1/2}$ spinor. These spinors are spin-pure to better than 1 part in 1000. For SnO, in which the spin-orbit interaction is of moderate strength, the ratios are close to 1:1 on the Sn atom and approximately 3:1 and 1:4 on the O atom for the $18e_{1/2}$ and $19e_{1/2}$ spinors. The $17e_{1/2}$ spinor still has the LS ratio. PbO has large spin-orbit interaction, and the $25e_{1/2}$ and $26e_{1/2}$ spinors have either $p_{1/2}$ on O with $p_{3/2}$ on Pb or vice versa. Even the $24e_{1/2}$ spinor has a 1:1 $p_{1/2} : p_{3/2}$ ratio on the O atom. The $25e_{1/2}$ and $26e_{1/2}$ spinors have almost equal α and β spin densities. The smaller $6p_{3/2}$ population in the $25e_{1/2}$ spinor compared to the $6p_{1/2}$ population in the $26e_{1/2}$ spinor reflects the promotion cost from the $6p_{1/2}$ to the $6p_{3/2}$ atomic spinor.

A further possible source of spin-orbit effects is the underlying d shell, which has a larger spin-orbit splitting than the valence p shell, and which is close in



energy to the O $2s$ shell. Despite this near-degeneracy and the resultant mixing of the atomic spinors that induces non-statistical $5d_{3/2}:5d_{5/2}$ ratios in the molecular spinors, the sum over the three relevant $\omega = 1/2$ spinors gives the statistical ratio, and there is no net spin-orbit effect on the molecule from the $5d$ shell.

The nonrelativistic Mulliken gross populations are given in Table VII. Comparison with the DHF populations shows a slight relativistic decrease in the atomic charges, a small decrease in the metal s population and increase in the O s population, with corresponding changes in the p populations. At first sight, the decrease in the metal s population is counter to the expected effect of relativity. The contributions from the individual orbitals (or spinors) gives some insight into this effect. The lower of the valence σ orbitals is principally a bonding combination between the metal s orbital and the O $2p\sigma$ orbital, and the higher orbital an antibonding combination with an sp hybrid on the metal polarized away from the O atom. Due to the relativistic stabilization of the metal s orbital, its contribution to the lower σ orbital increases. Consequently, its contribution to the higher σ orbital decreases, with the overall effect of decreasing the total metal s population. The effect is more pronounced for PbO than the lighter oxides. The spin-orbit stabilization of the $6p_{1/2}$ spinor in Pb assists in the transfer of charge from the $6s$. Since the $6p_{1/2}$ is $\frac{1}{3}\sigma$ and $\frac{2}{3}\pi$, there is a greater Pb π population in the $e_{1/2}$ spinors than in the nonrelativistic π orbitals. This is offset to some extent by a decrease in the Pb π population in the $e_{3/2}$ spinor. There is also a greater π population on the metal for SnO and GeO. This is reflected in the orbital eigenvalues which are given in Table VIII: the π eigenvalues are higher by 0.5eV at the DHF level.

B. RECP results.

The bond lengths of the monoxides predicted by the RECP calculations are nearly all substantially different from the all-electron values. The exceptions are the CER+ d value for SnO and the CER value for PbO, which are close to the all-electron values. These two potentials also gave good results for the hydrides. For PbO the CER+ d r_e value is too long by nearly 0.10Å, and the HW value is too short by the same amount. Over half the bond lengths have discrepancies with the all-electron

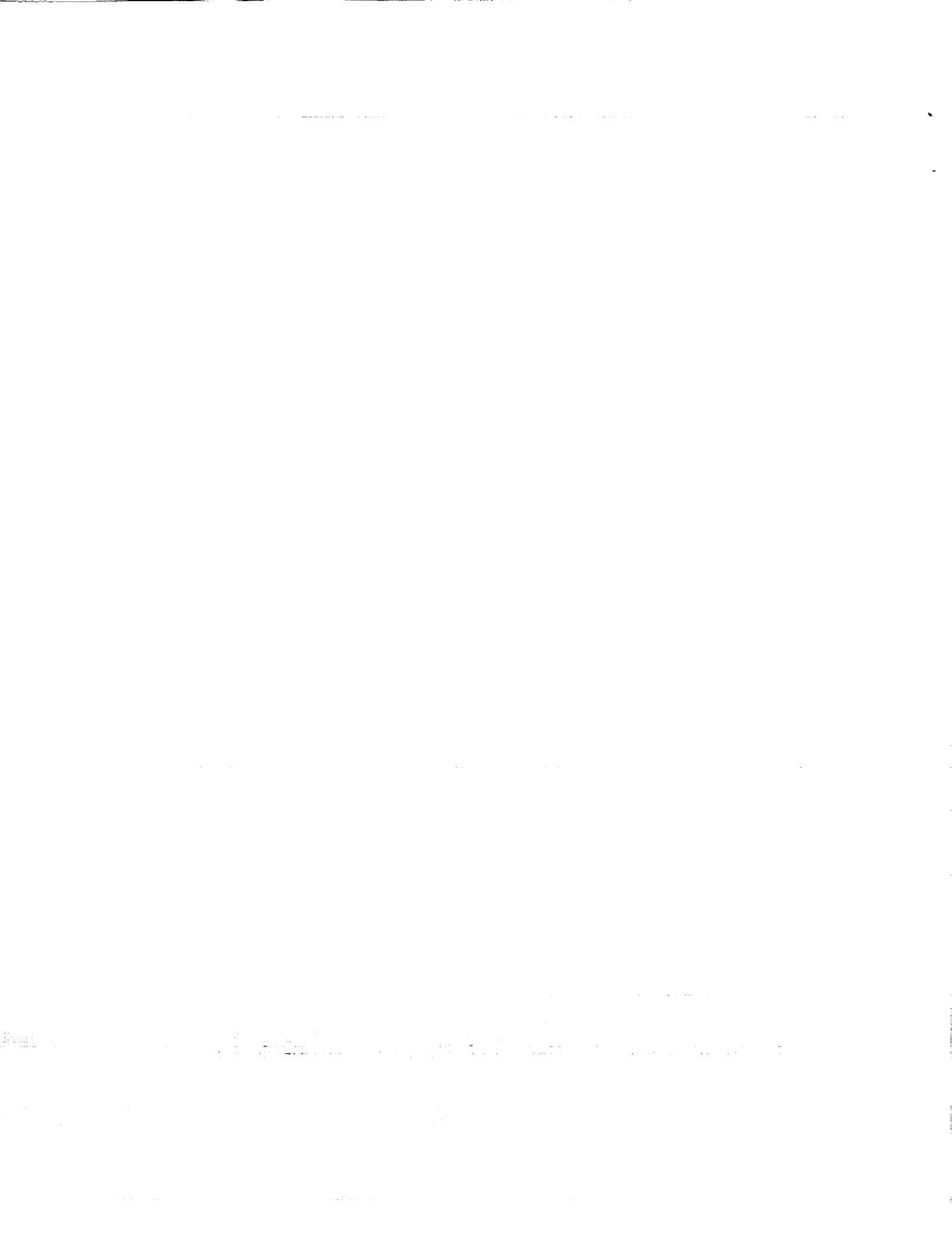
values which are greater than 0.03\AA . The most consistent results were obtained with the inclusion of the d shell (in the CER+ d RECP), with the exception for PbO just noted. Use of the valence basis from the all-electron calculations in place of the supplied basis had little effect on the results except for the SKBJ potentials, for which the supplied basis is quite different from the all-electron basis. Even so, the basis set changes are not sufficient to bring the results into agreement with the all-electron results.

Deviations from the all-electron dipole moments are also apparent in the RECP results. For GeO and SnO, the values are within 0.2 D of the all-electron PT value and mostly smaller, but for PbO they are greater by 0.4–0.6 D. The apparently better agreement with the PT value of the HW dipole moment for PbO is due to the underestimation of the bond length. Scaling the HW μ_e by the ratio of the PT and HW r_e values yields a value of 6.058, which is in the same range as those of the other RECPs. (A calculation with the HW RECP at the PT bond length gives a value of 6.386 D). The underestimation of the dipole moment is related to the underestimation of the bond length in many cases, and a similar scaling brings the values closer to the all-electron result. 6.386

The harmonic frequencies and IR intensities show similar patterns of deviation from the all-electron results to the stretching mode data of the hydrides. The frequencies and intensities are underestimated without the d shell explicitly treated in the calculations. The frequency differences are only 10cm^{-1} for GeO but range up to 50cm^{-1} for PbO. The underestimation of the frequencies in the RECP calculations may give a false impression of the importance of the spin-free and spin-orbit terms if the results for PbO were compared with experiment and with nonrelativistic all-electron calculations, without checking their accuracy by a proper calibration of the RECP. At the least, comparisons with PT results should be made to determine the range of error incurred in the RECP approximation.

C. Comparison with other results.

The RECP results of Igel-Mann *et al.* [25] on SnO and Basch *et al.* [20]



on PbO are generally in good agreement with the all-electron data presented here. Although the basis sets are a little different, they are of essentially the same quality. Basch *et al.* use Slater basis functions in their calculations rather than Gaussians. The RECP of Igel-Mann *et al.* is a “full-core” RECP but has a core-polarization potential; the RECP of Basch *et al.* has the $5d$ orbital in the valence space, and can be labelled a “semi-core” potential. Both potentials thus include the effect of the outer core, which is important for a correct description of molecular properties [35]. The bond length obtained by Igel-Mann *et al.* for SnO is a little short and the frequency a little high, but the values obtained are better than those obtained from the full-core potentials without the core polarization term. The results of Basch *et al.* are in good agreement with the all-electron results, with the exception of the IR intensity. This may in part be due to the coarser grid used to fit the dipole function around the minimum.

The minimum Slater basis set bond length of Schwenzler *et al.* [21] is shorter than the present value by 0.04\AA , as might be expected from a basis without polarization or diffuse functions. The harmonic frequency is in good agreement with the present value, but given the discrepancy in the bond length this must be considered fortuitous. The ECP results of Datta *et al.* [22] show close agreement with the all-electron values for the bond lengths, both relativistic and nonrelativistic, despite the lack of polarization functions, but the harmonic frequencies are much too low. Their ECPs do not take the core polarizability into account in any form: if they did, the bond length and the frequencies should be larger. The conclusion that they draw regarding the basis set deficiency in the calculations of Schwenzler *et al.* [21] is unjustified, since the standard for the evaluation of SCF molecular properties should be the basis-set limit all-electron SCF results, not experiment.

IV. CONCLUSIONS

Spin-orbit effects are increasingly important as one goes down the periodic table, as shown in the calculations on the group IV monoxides. While for GeO, PT is adequate to describe the relativistic effects, for SnO spin-orbit effects are

sufficiently important to affect the properties noticeably, and for PbO they are so important that their omission may cause serious errors in the predicted properties. The large spin-orbit interaction in Pb gives rise to bonding between $p_{1/2}$ spinors on one centre and $p_{3/2}$ spinors on the other, rather than hybridizing the relativistic spinors on each centre to form $p\sigma$ and $p\pi$ bonds with pure spin.

Several sets of RECPs were calibrated against the all-electron calculations. Similar trends to those found for the hydrides were noted in the molecular properties, with larger deviations from the all-electron values. None of the sets of RECPs gave consistent deviations. The high quality of the CER+ d RECP for Sn was confirmed, as was the poor quality of the CER+ d and the HW RECPs for Pb. Calibration of the results of RECP calculations against equivalent all-electron molecular calculations is essential for their use in high accuracy applications, and to avoid false conclusions drawn on the basis of comparison with experiment.

ACKNOWLEDGEMENTS

The author was supported by NASA grant NCC2-552, and would like to thank colleagues at NASA Ames Research Center for useful discussions.

REFERENCES

- [1] P. Chaix and D. Iracene, *J. Phys. B* **22**, 3791, 3815 (1989).
- [2] J. C. Phillips and L. Kleinman, *Phys. Rev.* **116**, 287 (1959).
- [3] L. Kahn, P. Baybutt, and D. G. Truhlar, *J. Chem. Phys.* **65**, 3826 (1976).
- [4] R. D. Cowan and D. C. Griffin, *J. Opt. Soc. Am.* **66**, 1010 (1976).
- [5] P. J. Hay and W. R. Wadt, *J. Chem. Phys.* **82**, 270, 284, 299 (1985).
- [6] W. J. Stevens, M. Krauss, H. Basch, and P. G. Jasien, *Can. J. Chem.*, in press.
- [7a] M. M. Hurley, L. F. Pacios, P. A. Christiansen, R. B. Ross, and W. C. Ermler, *J. Chem. Phys.* **84**, 6840 (1986).
- [7b] L. A. LaJohn, P. A. Christiansen, R. B. Ross, T. Atashroo, and W. C. Ermler, *J. Chem. Phys.* **87**, 2812 (1987).
- [7c] R. B. Ross, J. M. Powers, T. Atashroo, W. C. Ermler, L. A. LaJohn, and P. A. Christiansen, *J. Chem. Phys.* **93**, 6654 (1990).
- [8] Y Bouteiller, C. Mijoule, M. Nizam, J. C. Barthelat, J. P. Daudey, M. Pelissier, and B. Silvi, *Mol. Phys.* **65**, 295 (1988).
- [9] G. B. Bachelet, D. R. Hamann, and M. Schlüter, *Phys. Rev. B* **26**, 4199 (1982).
- [10] R. L. Martin, *J. Phys. Chem.* **87**, 730 (1983).
- [11] B. A. Hess, *Phys. Rev. A* **33**, 3742 (1986).
- [12] R. Samzow and B. A. Hess, *Chem. Phys. Lett.* **184**, 491 (1991).
- [13] P. J. C. Aerts and W. C. Nieuwpoort, *Int. J. Quantum Chem. Symp.* **19**, 267 (1986).
- [14] O. Visser, P. J. C. Aerts, and L. Visscher, in *The effects of relativity in atoms, molecules and the solid state*, edited by I. P. Grant, B. Gyorffy, and S. Wilson (Plenum: New York, 1991), p. 185.
- [15] K. G. Dyall, K. Fægri, Jr., and P. R. Taylor, in *The effects of relativity in atoms, molecules and the solid state*, edited by I. P. Grant, B. Gyorffy, and S. Wilson (Plenum: New York, 1990), p. 167.
- [16] O. Visser, L. Visscher, P. J. C. Aerts and W. C. Nieuwpoort, *J. Chem. Phys.* **96**, 2910 (1992).
- [17] K. G. Dyall, K. Fægri, Jr., P. R. Taylor, and H. Partridge, *J. Chem. Phys.* **95**, 2583 (1991).

- [18] K. G. Dyall, *J. Chem. Phys.* **96**, 1210 (1992).
- [19] K. P. Huber and G. Herzberg, *Molecular Structure and Molecular Spectra IV. Constants of Diatomic Molecules*, (van Nostrand Reinhold: New York, 1979)
- [20] H. Basch, W. J. Stevens, and M. Krauss, *J. Chem. Phys.* **74**, 2416 (1981).
- [21] G. M. Schwenzler, D. H. Liskow, H. F. Schaefer III, P. S. Bagus, B. Liu, A. D. McLean, and M. Yoshimine, *J. Chem. Phys.* **58**, 3181 (1973).
- [22] S. N. Datta, C. S. Ewig, and J. R. van Wazer, *Chem. Phys. Lett.* **57**, 83 (1978).
- [23] K. Balasubramanian and K. S. Pitzer, *J. Phys. Chem.* **87**, 4857 (1983).
- [24] K. Balasubramanian and K. S. Pitzer, *Chem. Phys. Lett.* **100**, 273 (1983).
- [25] G. Igel-Mann, C. Feller, H.-J. Flad, A. Savin, H. Stoll, and H. Preuss, *Mol. Phys.* **68**, 209 (1989).
- [26] F. B. van Duijneveldt, IBM Research Report RJ945 (1971).
- [27] T. H. Dunning, Jr., *J. Chem. Phys.* **90**, 1007 (1989).
- [28] K. G. Dyall, I. P. Grant, C. T. Johnson, F. A. Parpia, and E. P. Plummer, *Computer Phys. Commun.* **55**, 425 (1989).
- [29] INTDER: a program which performs curvilinear transformations between internal and Cartesian coordinates, written by W. D. Allen.
- [30] MOLECULE-SWEDEN is an electronic structure program system written by J. Almlöf, C. W. Bauschlicher, M. R. A. Blomberg, D. P. Chong, A. Heiberg, S. R. Langhoff, P.-Å. Malmqvist, A. P. Rendell, B. O. Roos, P. E. M. Siegbahn, and P. R. Taylor.
- [31] K. G. Dyall, *Chem. Phys. Lett.*, in press.
- [32] K. S. Pitzer, *J. Chem. Phys.* **63**, 1032 (1975).
- [33] P. A. Christiansen and K. S. Pitzer, *J. Chem. Phys.* **74**, 1162 (1981).
- [34] N. C. Pyper, *Chem. Phys. Lett.* **74**, 554 (1980).
- [35] L. G. M. Petterson, U. Wahlgren, and O. Gropen, *Chem. Phys.* **80**, 7 (1983).

TABLE I. Bond length r_e and relativistic correction to the bond length $\Delta^{rel}r_e$ of the XO molecules in Å. HW: results using Hay and Wadt [5] RECPs. CER: results using RECPs from Ref. 7; + d : with outer-core d shell in calculations. SKBJ: results using Stevens *et al.* [6] RECPs. Experimental results are from Huber and Herzberg [19].

	GeO	SnO	PbO
r_e			
HF	1.597	1.808	1.907
PT	1.593	1.797	1.871
DHF	1.594	1.801	1.893
Supplied basis contracted [3s3p]			
HW	1.577	1.739	1.776
CER	1.559	1.723	1.893
CER+ d	1.580	1.796	1.967
SKBJ	1.560	1.750	1.856
All-electron valence basis			
HW	1.580	1.736	1.776
CER	1.561	1.719	1.892
CER+ d	1.581	1.792	1.965
SKBJ	1.569	1.746	1.859
Other		1.78 ^a	1.864 ^b
Expt.	1.625	1.833	1.922
$\Delta^{rel}r_e$			
Pert.	-0.0040	-0.0113	-0.0363
DHF	-0.0030	-0.0074	-0.0146

^a Igel-Mann *et al.*, ref. 25.

^b Basch *et al.*, ref. 20.



TABLE II. Dipole moments μ_e and relativistic corrections to the dipole moments $\Delta^{rel}\mu_e$ of XO molecules in Debye. HW: results using Hay and Wadt [5] RECPs. CER: results using RECPs from Ref. 7; + d : with outer-core d shell in calculations. SKBJ: results using Stevens *et al.* [6] RECPs. Experimental results are from Huber and Herzberg [19].

	GeO	SnO	PbO
μ_e			
HF	4.076	5.153	5.598
PT	4.101	5.160	5.588
DHF	4.107	5.212	5.389
Supplied basis contracted [3s3p]			
HW	4.079	5.182	5.750
CER	4.005	5.003	6.197
CER+ d	3.961	5.124	6.193
SKBJ	4.002	5.133	6.044
All-electron valence basis			
HW	4.093	5.073	5.711
CER	4.000	4.873	6.160
CER+ d	3.964	4.974	6.151
SKBJ	4.082	5.023	6.003
Other			5.431 ^a
Expt.	3.272	4.32	4.64 ^b
$\Delta^{rel}\mu_e$			
PT	+0.025	+0.007	-0.010
DHF	+0.032	+0.059	-0.209

^a Evaluated from the SCF dipole moment function of Basch *et al.*, ref. 20.

^b μ_0 value.



TABLE III. Harmonic frequencies in cm^{-1} and infrared intensities in km mol^{-1} of XO molecules. Intensities are given in parentheses after frequencies. HW: results using Hay and Wadt [5] RECPs. CER: results using RECPs from Ref. 7; $+d$: with outer-core d shell in calculations. SKBJ: results using Stevens *et al.* [6] RECPs. Experimental results are from Huber and Herzberg [19].

	GeO	SnO	PbO
NR	1127(129)	955(128)	873(131)
PT	1124(134)	954(136)	867(174)
DHF	1123(133)	946(136)	785(66)
Supplied basis contracted [3s3p]			
HW	1113(114)	928(114)	819(130)
CER	1118(116)	940(112)	818(135)
CER+ d	1137(134)	949(144)	834(166)
SKBJ	1105(109)	920(114)	835(134)
All-electron valence basis			
HW	1110(115)	937(115)	818(131)
CER	1116(120)	952(112)	819(135)
CER+ d	1136(133)	961(145)	835(167)
SKBJ	1104(121)	930(115)	846(137)
Other		971 ^a	860(105) ^b
Expt	987	815	721

^a Igel-Mann *et al.*, ref. 25.

^b Evaluated from the SCF energy and dipole moment functions of Basch *et al.*, ref. 20.

TABLE IV. Spinor and orbital eigenvalues in eV of the Ge, Sn, Pb and O atoms.

	Relativistic		Nonrelativistic			
Ge	$3d_{3/2}$	-44.05	$3d$	-44.49		
	$3d_{5/2}$	-43.39				
	$4s_{1/2}$	-15.52			$4s$	-15.16
	$4p_{1/2}$	-7.42			$4p$	-7.33
	$4p_{3/2}$	-7.24				
Sn	$4d_{3/2}$	-36.36	$4d$	-37.38		
	$4d_{5/2}$	-35.22				
	$5s_{1/2}$	-13.88			$5s$	-13.04
	$5p_{1/2}$	-7.01			$5p$	-6.76
	$5p_{3/2}$	-6.57				
Pb	$5d_{3/2}$	-30.99	$5d$	-33.32		
	$5d_{5/2}$	-28.20				
	$6s_{1/2}$	-15.41			$6s$	-12.48
	$6p_{1/2}$	-7.49			$6p$	-6.53
	$6p_{3/2}$	-5.99				
O	$2s_{1/2}$	-34.08	$2s$	-34.02		
	$2p_{1/2}$	-16.78	$2p$	-16.77		
	$2p_{3/2}$	-16.75				



TABLE V. Mulliken population analysis of the valence spinors of XO molecules at τ_e . The d populations have been omitted, as they make little contribution to the valence populations or to the charges. Charges are given relative to the LS -coupled limit $(p_{1/2})^{4/3}(p_{3/2})^{8/3}$ for O, and for Ge, Sn and Pb they are given relative to the jj -coupled limit $(p_{1/2})^2$.

	X					O					Total	
	$s_{1/2}$	$p_{1/2}$	$p_{3/2}$	p	Total	$s_{1/2}$	$p_{1/2}$	$p_{3/2}$	p	Total		
GeO												
12e _{1/2}	1.03	0.00	0.01	0.01	1.04	0.15	0.28	0.52	0.80	0.96		
13e _{1/2}	0.00	0.20	0.10	0.30	0.35	0.00	1.10	0.54	1.64	1.65		
14e _{1/2}	0.60	0.23	0.40	0.62	1.24	0.09	0.22	0.46	0.67	0.76		
5e _{3/2}			0.28	0.28	0.34			1.65	1.65	1.66		
Charge	+0.27	+1.55	-0.83	+0.71	+0.87	-0.02	-0.28	-0.54	-0.82	-0.87		
SnO												
17e _{1/2}	1.13	0.01	0.02	0.02	1.16	0.10	0.28	0.46	0.74	0.84		
18e _{1/2}	0.02	0.15	0.13	0.28	0.34	0.00	1.21	0.45	1.65	1.66		
19e _{1/2}	0.57	0.29	0.30	0.59	1.16	0.04	0.17	0.63	0.79	0.84		
8e _{3/2}			0.23	0.23	0.28			1.72	1.72	1.72		
Charge	+0.23	+1.54	-0.70	+0.84	+0.98	-0.00	-0.34	-0.62	-0.96	-0.98		
PbO												
24e _{1/2}	1.39	0.01	0.02	0.03	1.43	0.10	0.24	0.23	0.47	0.57		
25e _{1/2}	0.24	0.00	0.25	0.25	0.53	0.01	1.45	0.01	1.46	1.47		
26e _{1/2}	0.11	0.72	0.03	0.75	0.88	0.03	0.04	1.04	1.08	1.12		
13e _{3/2}			0.14	0.14	0.18			1.82	1.82	1.83		
Charge	+0.17	+1.25	-0.46	+0.79	+0.91	+0.01	-0.43	-0.48	-0.90	-0.91		

TABLE VI. DHF integrated spin densities for the valence spinors (Kramers pairs) of the XO molecules at r_e . The values shown are for the $e_{1/2}$ and $e_{-3/2}$ spinors. The time-reversed spinors $e_{-1/2}$ and $e_{3/2}$ have the same densities with opposite spin. The densities represent the occupation number of the orbital whose symmetry type given at the head of the column. The sum is taken over spin for all occupied valence spinors.

		$\sigma(\alpha)$	$\pi(\beta)$
GeO			
	$12e_{1/2}$	1.000	0.000
	$13e_{1/2}$	0.000	1.000
	$14e_{1/2}$	1.000	0.000
	$5e_{-3/2}$		1.000
	Sum	4.000	4.000
SnO			
	$17e_{1/2}$	0.999	0.001
	$18e_{1/2}$	0.015	0.985
	$19e_{1/2}$	0.984	0.016
	$8e_{-3/2}$		1.000
	Sum	3.996	4.004
PbO			
	$24e_{1/2}$	0.992	0.008
	$25e_{1/2}$	0.432	0.568
	$26e_{1/2}$	0.538	0.462
	$13e_{-3/2}$		1.000
	Sum	3.926	4.074



TABLE VII. Nonrelativistic Mulliken gross population analysis of the valence orbitals of the XO molecules at r_e . The d populations have been omitted, as they make little contribution to the valence populations or to the charges.

	X			O		
	<i>s</i>	<i>p</i>	Total	<i>s</i>	<i>p</i>	Total
GeO						
9 σ	0.91	0.01	0.92	0.15	0.93	1.08
10 σ	0.81	0.57	0.86	0.05	0.56	1.12
4 π		0.52	0.63		3.36	3.37
Charge	+0.18	+0.84	+0.91	+0.02	-0.90	-0.91
SnO						
12 σ	0.91	0.02	0.93	0.08	0.98	1.07
13 σ	0.92	0.49	1.42	0.00	0.59	0.59
6 π		0.45	0.55		3.44	3.46
Charge	+0.12	+1.00	+1.03	+0.05	-1.06	-1.03
PbO						
16 σ	1.10	0.01	1.12	0.06	0.82	0.88
17 σ	0.68	0.57	1.26	0.02	0.72	0.74
9 π		0.48	0.58		3.42	3.43
Charge	+0.15	+0.89	+0.96	+0.05	-1.00	-0.96



TABLE VIII. Spinor and orbital eigenvalues in eV of the XO molecules at r_e .

	Relativistic		Nonrelativistic	
GeO	$12e_{1/2}$	-16.92	9σ	-16.97
	$13e_{1/2}$	-12.35	4π	-12.80
	$5e_{3/2}$	-12.33		
	$14e_{1/2}$	-11.66	10σ	-11.69
SnO	$17e_{1/2}$	-15.21	12σ	-14.91
	$18e_{1/2}$	-11.01	6π	-11.54
	$8e_{3/2}$	-11.19		
	$19e_{1/2}$	-10.50	13σ	-10.47
PbO	$24e_{1/2}$	-16.21	16σ	-13.96
	$25e_{1/2}$	-11.36	9π	-10.61
	$13e_{3/2}$	-10.84		
	$26e_{1/2}$	-9.90	17σ	-9.91



First draft

Manuscript date: September 10, 1992

Journal for submission: J. Chem. Phys.

Relativistic effects on the bonding and properties of the hydrides of platinum.

Kenneth G. Dyall *,
Eloret Institute, 3788 Fabian Way, Palo Alto,
California 94303, U.S.A.

Abstract

The ground states of PtH^+ and PtH_2 and several low-lying states of PtH have been studied at the self-consistent field level of theory to determine the importance of relativistic effects. The results of calculations based on Dirac-Hartree-Fock theory, nonrelativistic theory and the spin-free no-pair relativistic approximation of Hess are compared to separate the effects of the spin-free terms and the spin-orbit terms in the relativistic corrections to the molecular properties. Comparison is also made between first-order perturbation theory including the one-electron spin-free terms and the Hess method to determine the size of effects beyond first order. It is found that the spin-orbit interaction significantly affects the properties and energetics of these molecules because of the participation of the Pt $5d$ orbital in the bonding. Any calculation on Pt compounds which does not explicitly include spin-orbit interaction cannot be considered reliable.

* Mailing address: NASA Ames Research Center, MS RTC 230-3, Moffett Field, CA 94035-1000, U.S.A.

I. INTRODUCTION

The combustion of hydrogen on platinum surfaces is an important area of catalytic chemistry. A number of calculations have been made on models of the dissociation of H_2 on Pt, treating from one to nine Pt atoms [A1-A16] at various levels of theory, most including some treatment of relativistic effects through the use of spin-averaged relativistic effective core potentials (RECPs), and most incorporating electron correlation effects in some way. It has been recognized that relativistic effects must be included in calculations on molecules containing heavy elements, but to what lengths it is necessary to go to include them is a question that still needs to be answered: for example, in the chemistry of the 6p block spin-orbit interaction is known to be important [A17-A19].

The aim of this work is to examine the question of the importance of both spin-free and spin-dependent (spin-orbit) relativistic effects for the hydrides of Pt. The effect of spin-orbit interaction is assessed by comparison of the DHF results with those from the "spin-free no-pair method correct to second-order in the external potential" of Hess *et al.* [A20,A21], hereafter designated PVP. This method is derived from the Dirac equation by a transformation decoupling the large and small components, and neglecting the spin-orbit terms. Since its Hamiltonian can be used in variational calculations, effects beyond first order in α^2 can be obtained. The effect of terms beyond first order are obtained by comparison of the PVP results with those from first-order perturbation theory (PT) including only the mass-velocity and Darwin (MVD) terms [A25,A26]. These are the spin-free relativistic corrections to the one-electron operator of order α^2 . The spin-free part of the relativistic correction is obtained by comparing the PVP and nonrelativistic results.

II. THEORY

The Dirac-Hartree-Fock program described previously [A27,A28] has been extended to perform Kramers-restricted open-shell calculations on doublet states, where the unpaired electron can be either a single electron outside or a hole inside

a closed-shell core, or a combination of several such particle or hole states. In the presentation of the theory and its implementation, the concepts of Hsu *et al.* [A29] and Fægri and Manne [A30] have been followed.

For a single electron outside a closed core, the closed-virtual and open-virtual Fock operators \hat{F}^{cv} and \hat{F}^{ov} are defined by

$$\begin{aligned}\hat{F}^{cv} &= \hat{F}^{core} + \frac{1}{2}\hat{F}_m^{open}, \\ \hat{F}^{ov} &= \hat{F}^{core},\end{aligned}\tag{1}$$

with

$$\begin{aligned}\hat{F}^{core} &= \hat{h} + \sum_{k=1}^{n_c} \hat{G}_k, \\ \hat{F}_m^{open} &= \hat{G}_m,\end{aligned}\tag{2}$$

where n_c is the number of closed-shell Kramers pairs of spinors (the relativistic equivalent of orbitals), and

$$\hat{G}_k = \hat{Q}_k + \hat{Q}_{\bar{k}}; \quad \hat{Q}_k = \hat{J}_k - \hat{K}_k\tag{3}$$

with \hat{J}_k and \hat{K}_k defined in the usual way but with respect to molecular spinors, and the bar indicating time-reversal applied to the specified spinor: spinors $|k\rangle$ and $|\bar{k}\rangle$ form a Kramers pair. The closed-open Fock operator is obtained from \hat{F}^{cv} and \hat{F}^{ov} [A30]:

$$\hat{F}^{co} = 2\hat{F}^{cv} - \hat{F}^{ov} = \hat{F}^{core} + \hat{F}_m^{open}.\tag{4}$$

Similarly, for state-averaged doublets,

$$\begin{aligned}\hat{F}^{cv} &= \hat{F}^{core} + \frac{1}{2n_o}\hat{F}^{open}, \\ \hat{F}^{ov} &= \hat{F}^{core}, \\ \hat{F}^{co} &= \hat{F}^{core} + \hat{F}^{open},\end{aligned}\tag{5}$$

where n_o is the number of open-shell Kramers pairs, and

$$\hat{F}^{open} = \sum_{m=n_c+1}^{n_c+n_o} \hat{F}_m^{open}.\tag{6}$$

For a single hole state, the same Fock operators may be used, but it is more convenient to express them in terms of a hole rather than a particle in the m th Kramers pair:

$$\begin{aligned}
\hat{F}^{cv} &= \hat{F}^{closed} - \frac{1}{2}\hat{F}_m^{open}, \\
\hat{F}^{ov} &= \hat{F}^{closed} - \hat{F}_m^{open}, \\
\hat{F}^{co} &= \hat{F}^{closed},
\end{aligned}
\tag{5}$$

where \hat{F}^{closed} now includes \hat{G}_m . For state-averaged doublet holes,

$$\begin{aligned}
\hat{F}^{cv} &= \hat{F}^{closed} - \frac{1}{2n_o}\hat{F}^{open}, \\
\hat{F}^{ov} &= \hat{F}^{closed}, \\
\hat{F}^{co} &= \hat{F}^{closed} - \frac{1}{2n_o-1}\hat{F}^{open}.
\end{aligned}
\tag{5}$$

The single Fock matrix method of Fægri and Manne [A30] has been employed in the present implementation, with the same choice of diagonal blocks. Hsu et al [A29] have argued that in order to ensure that the solution for a core hole state corresponds to an excited state, the diagonal core-core and open-open blocks of \mathbf{F} should be composed of the matrix elements of \hat{F}^{closed} . This has the effect of diagonalizing the CI matrix of single excitations involving all other core holes, and providing some bound to the energy of the core hole state. However, the choice of \hat{F}^{co} already ensures zero interactions with the other core hole states, and the choice of \hat{F}^{cc} and \hat{F}^{oo} remains arbitrary.

In the implementation of the open-shell doublet method, only two Fock operators need to be constructed, \hat{F}^{core} (or \hat{F}^{closed}) and \hat{F}^{open} . These are constructed in the scalar basis, as before, transformed to the 2-spinor basis and combined to form a single Fock operator. Advantage is taken in their construction of the fact that the same addresses are required in the gather/scatter operation for both Fock operators. In the present calculations on PtH, the extra time taken for the second Fock operator amounted to less than 20% of the time for the first Fock operator. The scheme for calculating the addresses has also been improved and time-reversal symmetry implemented in the construction of \mathbf{F} , resulting in a saving in CPU time of more than 30%.

III. COMPUTATIONAL DETAILS

Moderately large Gaussian basis sets have been used for Pt and H, so that the results should be close to the DHF limit. For Pt, the $22s\ 16p\ 13d\ 8f$ primitive basis set of Fægri [A31] was taken as a starting set. An extra s function was added to the valence space and the three outer s functions reoptimized. Three p and two d functions were added in an even-tempered series with ratio 0.4, and two f functions with exponents 0.2 and 0.08 were added for polarization of the $5d$ orbital. In the relativistic basis set an extra tight p function with exponent 6.8×10^5 was added to make up part of the deficiency in the $p_{1/2}$ space [A32]. The addition of this function lowered the DHF total energy by $0.5 E_h$, leaving a discrepancy of $0.152 E_h$ between it and the DHF limiting value, compared with $0.01 E_h$ for the nonrelativistic discrepancy. The core was generally contracted to $5s\ 4p\ 3d\ 1f$ using the atomic SCF orbitals, leaving a primitive valence set of $4s\ 4p\ 4d\ 2f$. For hydrogen a $3s\ 2p$ contracted set was used, taking the $5s$ primitive set of Huzinaga [A33] contracted to $3s$, and two p functions with exponents 1.25 and 0.45 [A34]. The relativistic contraction coefficients were obtained from an adaption of GRASP [A35] described previously [A28].

The results from nonrelativistic (NR), first-order perturbation theory (PT) and the PVP method were obtained with the MOLECULE/SWEDEN [A36] package. DHF results were obtained with the program described above. The value of the speed of light in atomic units was taken to be 137.0359895. SCF calculations for PtH and PtH⁺ were carried out at 5 internuclear separations around the minimum distance with a spacing of 0.1 Å. The energies were fit to a quartic function in the internuclear separation. SCF calculations for PtH₂ were carried out at 4 Pt-H distances around the minimum distance with a spacing of 0.07 Å and at 5 H-Pt-H angles around the minimum spaced at 2°. The energies were fit to a cubic function in the two coordinates. Infrared (ir) data were obtained with the program INTDER [A37] All calculations were performed on the Computational Chemistry CONVEX C-210 and Central Computing Facility CRAY Y-MP/864 computers at NASA Ames Research Center.

IV. RESULTS AND DISCUSSION

A. Pt atom

It has been pointed out by a number of authors [A16, A38] that in order to obtain the correct ordering of molecular states, it is necessary to have the correct ordering of the atomic states. This is particularly so for transition metal atoms where there are three configurations that contribute low-lying states to the atomic spectrum, viz. d^n , $d^{n-1}s$ and $d^{n-2}s^2$. These remarks have been made in the context of the inclusion of correlation effects. As well as correlation effects, for heavy atoms such as Pt, relativistic effects are of such great importance that a correct description of the atomic states cannot omit them. Many calculations which include relativistic effects via RECPs do not include spin-orbit effects, since these require considerable extra work. The comparisons with experiment made in these studies average over the J components of an LS term. A cursory examination of the levels of the d^9s configuration from the optical spectrum of Pt [A39] shows that electrostatic and spin-orbit interactions are of comparable magnitude. A correct description of the Pt atom will therefore have to take spin-orbit effects into account, and there is some doubt whether averaging over J values will give a meaningful term energy with which to compare, since the levels of a given LS multiplet do not obey the Landé interval rule.

The results of DHF calculations using GRASP [A35] on the $(d+s)^{10}$ configuration complex, followed by CI within the complex, are presented in Table I. The state designations are given in both jj and LS coupling. The effect of the Breit interaction and estimated quantum electrodynamic (QED) effects are also included. The strong configuration mixing makes the assignment of states to given terms difficult, and the multiplet designations given in the experimental spectrum may have to be revised. The J quantum number is the only reliable designator, and based on this, the calculated levels agree fairly well with the experimental levels, when the designation of the $d^8s^2\ ^3P_2$ and the $d^9s^1\ ^1D_2$ have been reversed. These two states are strongly mixed in any case, so that the labelling is somewhat academic. The results are sensitive to the weights of the three configurations used in the SCF

optimization, with the best overall results (given here) obtained with equal weights of the d^8s^2 and d^9s configurations, and 10% relative weight of the d^{10} configuration. However, use of the orbitals from an SCF calculation on the d^9s configuration lowered the energy of the d^{10} state by 10000 cm^{-1} while raising the d^8s^2 state energies by 5000 cm^{-1} ; using 1000% relative weight of the d^{10} configuration gave a d^{10} level energy of 5889 cm^{-1} , which is close to the experimental value of 6140 cm^{-1} . Clearly, a single orbital set cannot adequately describe all three configurations, and correlation effects, including orbital relaxation, must be included to obtain a more quantitative prediction of the energy levels. It is noteworthy that the inclusion of the Breit interaction made relative shifts of energy levels of up to 800 cm^{-1} , indicating that it must also be included for quantitative ("chemical") accuracy.

B. PtH⁺

Little is known about PtH⁺ experimentally. The ground state is asserted to be $^3\Delta$ by Wang and Pitzer [A3], which can have ω values of 1, 2 and 3. Balasubramanian's [A9] calculations at $3.1a_0$, which include both spin-orbit and electron correlation effects, show that the ground state has 0^+ symmetry and is dominated by the nonrelativistic $^1\Sigma^+$ configuration, but with a substantial contribution from the $^3\Pi$; the $^3\Delta_3$ is the next state, more than 4000 cm^{-1} higher in energy.

DHF calculations have been performed on the lowest 0^+ state of PtH⁺, and NR, PVP and PT calculations on the $^1\Sigma^+$, $^3\Pi$ and $^3\Delta$ states. The results, including basis set superposition error (BSSE) calculated by the counterpoise method [A40], are reported in Table II. The fragments for the interaction energies were taken to be Pt⁺ and H, justified by the ionization potentials (IPs) of H and Pt and by the Mulliken populations, given in Table III at $r = 3.1a_0$, which place most of the molecular charge on the Pt. Only the PT calculations were significantly affected by BSSE. The largest effect was a 20 cm^{-1} increase in the $^1\Sigma^+$ harmonic frequency, and the effects on D_e were less than 0.2 kcal mol^{-1} . At the NR ROHF level, the $^3\Pi$ and the $^3\Delta$ curves were repulsive in the vicinity of the $^1\Sigma^+$ minimum, but the $^3\Delta$ curve was less repulsive than the $^3\Pi$ curve. Addition of the mass-velocity and Darwin (MVD) terms stabilized all three states, but the $^3\Pi$ state still only had a shallow

minimum, at a value of r greater than $3.5a_0$. The stabilization can be related to the s population on Pt, from which the principal contribution of the MVD operator to the valence energy comes, and which is largest for the ${}^3\Delta$ state and smallest for the ${}^1\Sigma^+$ state. The stability of the states correlates with the amount of charge transfer from H to the Pt^+ ion. Electron correlation effects undoubtedly lower the ${}^1\Sigma^+$ state more than either of the triplet states, and from the current calculations and those of Balasubramanian it can be concluded that the ground state of PtH^+ is indeed the ${}^1\Sigma^+$ (0^+) state.

The changes to the bonding orbitals induced by relativity are illustrated by the DHF Mulliken gross populations at $r = 3.1a_0$, also given in Table III. The expansion of the Pt $5d$ orbital enables charge to be transferred from it to the relativistically stabilized Pt $6s$ and the H $1s$ orbitals. The latter transfer reduces the charge on H, making the molecule more like $\text{Pt}^+ - \text{H}$. The strong influence of spin-orbit interaction is shown by the breakdown of the DHF populations by spin-orbit components and spin densities, displayed in Table IV. Both valence spinors have almost equal contributions from α and β spin, a situation about as far from λ - s coupling as possible. The $20e_{1/2}$ spinor has almost no Pt $5d_{5/2}$ contribution, and the contributions to the $21e_{1/2}$ spinor from the two $5d$ spin-orbit components are by no means in the λ - s coupling ratio. The dominance in the MSs of one $5d$ spin-orbit component on Pt has an inductive effect on the H p spinors, forcing one of them to give a negligible contribution. This effect has been noted previously [A19], and occurs because the combination of spinors with opposite κ^* on two centres gives bonding functions in both α and β spin spaces, whereas combinations with the same κ give a bonding function for one spin with an antibonding functions for the other spin. Table IV also shows that the charge on the Pt atom is due to removal of an electron from a $5d_{5/2}$ spinor, with the rest of the charge transfer from the $5d$ shell distributed between both spin-orbit components.

The effect of spin-orbit interaction on the molecular properties can readily

* Quantum number of the relativistic angular operator $\hat{K} = -1 - 2\mathbf{S} \cdot \mathbf{L}$, which is related to the spin-orbit interaction.

be explained by the mixing of the ${}^3\Pi_{0+}$ state into the ${}^1\Sigma_{0+}^+$ state. The ${}^3\Pi_{0+}$ state has a larger bond length and smaller frequency, and the interaction between the two will increase D_e . The importance of spin-orbit interaction is shown by the size of the differences between the PT results and the DHF results: 0.02\AA in r_e , 120cm^{-1} in ω_e and 7.5kcal mol^{-1} in D_e . The extent of the mixing can be judged from the integrated spin densities, which show a $\sigma \rightarrow \pi$ promotion of $0.23e$. Clearly, spin-orbit effects cannot be ignored in this molecule.

It is necessary to exercise some degree of caution with the results of PT calculations involving the MVD terms. It has been shown for some transition metal compounds that the results of PT calculations are not stable with respect to the contraction scheme [A41]. A systematic study of the effect of core orbital relaxation on the $d^{10} {}^1S \rightarrow d^9 s {}^3D$ excitation energy of Pd was made by Blomberg and Wahlgren [A42], in which they showed that the relaxation of the outer core orbitals was necessary to obtain consistent PT results. In contrast, neither the NR SCF nor the no-pair approximation of Almlöf *et al.* [A43] showed much dependence of the excitation energy on the core relaxation. A series of calculations was performed to assess the effect of contraction on the properties of PtH⁺ at the NR and PT levels of theory. The valence basis was increased by uncontracting the outermost primitive functions from the core, one at a time, until the properties stabilized. When the second s and p functions were uncontracted the core parts of the $5s$ and $5p$ were discarded for reasons of linear dependence. The results are given in Table V. The most dramatic change in the PT properties occurred with the uncontraction of the first s function — a not unreasonable result, considering the nature of the mass-velocity and Darwin operators. Given the changes, the PT results reported in Table II are for the $5s5p5d$ valence basis. The very small changes in the NR values, coupled with the experience of Blomberg and Wahlgren, give grounds for confidence that the DHF results are stable. Gropen *et al.* [A16], in their calculations on PtH, have also found that a flexible valence basis is necessary when using PT.

C. PtH

Spin-orbit effects are dominant for this molecule, and the structure of the

low-lying states cannot be understood without it. In λ - s coupling there are three terms that arise from the d hole on Pt, ${}^2\Delta$, ${}^2\Pi$ and ${}^2\Sigma^+$. The first two are split by spin-orbit effects to give ${}^2\Delta_{5/2}$, ${}^2\Delta_{3/2}$, ${}^2\Pi_{3/2}$, and ${}^2\Pi_{1/2}$ states. The ${}^2\Delta_{3/2}$ and ${}^2\Pi_{3/2}$ states are mixed by the spin-orbit interaction as are the ${}^2\Pi_{1/2}$ and ${}^2\Sigma_{1/2}^+$. In ω - ω coupling there are two sets of states, arising from the $5d_{5/2}$ and $5d_{3/2}$ holes on Pt, the former having $\omega = 5/2, 3/2$ and $1/2$ and the latter having $\omega = 3/2$ and $1/2$, the former correlating with the atomic states $[5d_{5/2}]6s^1 J = 3, 2^*$, designated in LSJ coupling as 3D_3 and 3D_2 , and the latter correlating with the atomic states $[5d_{3/2}]6s^1 J = 2, 1$, designated in LS coupling as 1D_2 and 3D_1 . The results of three sets of calculations are presented in Table VI, a 5-state average DHF calculation, a 3-state average DHF calculation and separate calculations on the the lowest three states. The 5-state average calculation clearly shows the grouping of the molecular states based on the jj -coupled hole states: the two groups are separated by the $5d$ spin-orbit splitting of about 10000 cm^{-1} . The importance of the spin-orbit splitting is also reflected in the molecular properties. The $5/2$ and $3/2(1)$ states, which in λ - s coupling would be spin-orbit components of the ${}^2\Delta$ state, have significantly different bond lengths, harmonic frequencies and dipole moments. The differences are too large for a small perturbation. There is more similarity between the $3/2(1)$ and $1/2(1)$ states, which are not components of a spin-orbit doublet. The differences in the molecular properties also cast doubt on any procedure which includes the spin-orbit splitting as a constant shift applied to the non-relativistic curves (or even curves obtained with RECPs) on the basis that the splitting is local to the heavy atom. The involvement of the spin-orbit split orbital in bonding undermines the assumption of locality.

The results of the NR and PT calculations are presented in Table VII. Similar problems with the PT calculations were encountered as for PtH^+ . Results for both the $4s4p4d$ and $5s5p5d$ valence basis sets are reported. The seriousness of the errors incurred with the more highly contracted basis is emphasized by the fact that the predicted ground state changes when the basis is uncontracted. The importance of relativistic effects in stabilizing the molecular states is obvious. At the NR SCF

* The square brackets indicate a hole in a filled shell

level, only the $^2\Sigma^+$ state is bound. However, comparison of the PT results with the DHF results shows that the omission of the spin-orbit interaction is at least as serious as the omission of the non-fine-structure terms. The spread of states is only 3000cm^{-1} , which is similar to the spread of states based on the $5d_{5/2}$ hole in the DHF calculations. Thus the valence electrostatic interactions are only a third of the size of the spin-orbit splitting.

The Mulliken gross populations are presented in Tables VIII and IX. The most significant difference between the NR and DHF populations is the transfer of charge from the d shell into the s shell. It is noteworthy that the atomic charges of the $5/2$ and $3/2$ states is lower than that of the $^2\Delta$ and $^2\Pi$ states, but the $1/2$ state has the same charges as the $^2\Sigma^+$ state.

Further evidence for the importance of spin-orbit effects in determining the state designations is obtained from the atomic spinor contributions to the Mulliken populations and the integrated spin densities of the valence MSs. These are presented in Tables X and XI. If the molecule is well-described in the λ - s coupling scheme, the ratio of the $j = \ell + 1/2$ and $j = \ell - 1/2$ component densities should be $\ell + m + 1 : \ell - m$ for spinors with $\omega = m + 1/2$ for pure α spin, and the reverse for pure β spin. Few of the spinors have ratios that are close to these values. The integrated spin densities are perhaps a better indication of the mixing. The $20e_{1/2}$ and $22e_{1/2}$ spinors are mostly σ and the $21e_{1/2}$ mostly π , but with strong mixing, especially for the $1/2$ state. The sums of the densities give the orbital occupation numbers. While the $5/2$ state is very close to a pure δ hole state, the $3/2$ state has a strong mixing of the π and δ holes, and the $1/2$ state a smaller but still significant mixing of the σ and π holes.

There has been a number of previous calculations on PtH [A1,A3,A8,A13,A16], mainly in connection with the $^2\Delta - ^2\Sigma^+$ separation. Wang and Pitzer [A3] report RECP SCF calculations, and examine the effect of spin-orbit interaction via CI and correlation via singles and doubles (SD)CI calculations. With the spin-orbit interaction but without correlation, the $1/2(1)$ and $3/2(1)$ states have excitation energies of -1229 cm^{-1} and 4082 cm^{-1} relative to the $5/2$ state; correlation changes these

to 1008 cm^{-1} and 2742 cm^{-1} . The $1/2(2)$ state is 11810 cm^{-1} above the $1/2(1)$ state, but the $3/2(2)$ state is 19350 cm^{-1} higher than the $3/2(1)$ state. These calculations, while they demonstrate the importance of the spin-orbit interaction, clearly have some deficiencies. Rohlfiing *et al.* have performed a systematic set of RECP calculations on the states of NiH, PdH and PtH, incorporating correlation by Møller-Plesset (MP) perturbation theory up to fourth order. Their results demonstrate the importance of inclusion of the semi-core $5s$ and $5p$ orbitals on Pt in the valence space, particularly when electron correlation is included. The correlated results show a remarkably small change in the excitation energies of the ${}^2\Delta$ and ${}^2\Pi$ states. Their UHF results have been included in Table ? for comparison with the present ROHF results. The properties display significant deviations from the PT and the PVP results — shorter bond lengths, higher harmonic frequencies and dissociation energies. Although their valence basis set is somewhat smaller, it does contain an f function on Pt and a p function on H, and should not give results too different from the basis used in this work. If the contraction of the bond length due to correlation for the ${}^2\Delta$ state obtained by them is applied to the DHF results, the bond length $5/2$ state is in very good agreement with the experimental value of 1.5285Å . Nevertheless, the results of Rohlfiing *et al.* [A8] for T_e using a simple model of the spin-orbit splitting are in reasonable agreement with the present values.

D. PtH₂

The equilibrium geometries, dipole moments and energies for dissociation into Pt 1S_0 and H₂ are presented in Table XII. No nonrelativistic (NR) SCF results are given because at this level, PtH₂ is unbound — except perhaps for a van der Waals minimum between the Pt atom and the H₂ molecule. This is not surprising, since the nonrelativistic ground configuration of Pt atom is d^{10} , a closed-shell configuration. The energy required to break up a closed-shell configuration by promotion into the next unoccupied orbital is usually too high for the formation of strong bonds, and such atoms tend to form van der Waals complexes. For Pt, the $d-s$ promotion energy is considerably reduced by the lowest order relativistic effects, so that the inclusion of PT makes PtH₂ stable with respect to both the d^{10} and the

ground state $d^9 s^1 {}^3D$ Pt atom asymptotes, in the latter case by 3.5kcal mol^{-1} .

What is required is promotion of an electron from the d orbital into the empty s orbital [A5,A6]. Relativistic effects stabilize the s orbital and destabilize the d orbital sufficiently for Pt that the ground configuration is $d^9 s^1$. The s orbital stabilization is already obtained with PT, and the molecule is stabilized by 15kcal mol^{-1} relative to the d^{10} asymptote, and is still bound by 3.5kcal mol^{-1} relative to the ground $d^9 s^1 {}^3D$ state of Pt and H_2 .

There is some little confusion over the issue of the bonding in PtH_2 . In his conclusions, Balasubramanian [A9] predicts that "the $\text{Pt}({}^1S_0)$ state would insert into H_2 almost spontaneously to form the bent PtH_2 ground state while the 3D_3 state would not react with H_2 spontaneously". These conclusions are based on RECP/CASSCF/CI calculations which show only a small barrier in the 1A_1 surface to the insertion, but a large barrier in the 3A_1 surface, with a linear equilibrium geometry and a higher energy than the asymptote. The Mulliken populations he gives indicate a substantial Pt $6s$ population ($0.75e$), which suggests that $d-s$ promotion is necessary for bonding, a conclusion arrived at by Low and Goddard [A5,A6]. Since the ground state of PtH_2 is (in LS coupling) a singlet, its formation must occur from a singlet state of the atom. When spin-orbit interaction is introduced, this requirement is removed. However, dissociation of PtH_2 at the Dirac-Fock level must still occur to a state of the atom in which all electrons are paired, and the lowest such state is the d^{10} state. As the dissociation limit is approached, the curve for this state must undergo avoided crossings with triplet states arising from the $d^9 s^1 {}^3D_3$, $d^9 s^1 {}^3D_2$ and $d^8 s^2 {}^3F_4$ asymptotes, all of which can contribute a molecular state with A_1 double-group symmetry.

Spin-orbit effects have a marked impact on the geometry. The DHF bond angle is nearly 5° greater than the PT bond angle. This is much larger than the difference for PbH_2 [A18], which was only 1° . The analysis of the electron density into contributions from the single-group irreps gives insight into this increase in bond angle. In the valence region, electron density is transferred by spin-orbit effects into the b_1 component from all the others, but mainly from the a_1 component. The

greater density in the b_1 component increases the repulsion between the bonding pairs which increases the bond angle.

Such an increase in bond angle due to spin-orbit effects has important implications for the dissociation of H_2 on Pt surfaces. Sjøvoll's [A15] calculations on Pt_9H_2 indicate that the dissociated H_2 molecule in fourfold hollow sites on the 100 surface is less stable than the locally PtH_2 -like configuration. Spin-orbit effects, in opening up the bond angle, would then facilitate the dissociation of H_2 into a chemisorbed state. Moreover, the lowering of symmetry due to the spin-orbit interaction may remove the necessity for preparing the cluster for bonding to H_2 : in C_{2v} symmetry there is only one fermion double-group irreducible representation (irrep), so that the MSs can freely change their composition in terms of single-group basis functions.

The bond angle obtained in the PT calculations is similar to the value obtained by Sjøvoll [A15], but smaller than that obtained by Balasubramanian [A9]. Both these calculations employed RECPs and included correlation via CASSCF/MRCI calculations. Sjøvoll's basis included f functions and had the $4d$, $5s$ and $5p$ semi-core orbitals frozen, where Balasubramanian's had no f functions and no frozen semi-core orbitals.

IV. CONCLUSIONS

Strong spin-orbit effects are evident in the hydrides of Pt. The grouping of the low-lying states of PtH is determined by the large Pt atomic $5d$ spin-orbit splitting, and the potential energy curves are not parallel, as might be expected if spin-orbit effects were small. The geometries and harmonic frequencies of the states PtH^+ and PtH are significantly altered by spin-orbit effects; the bond angle in PtH_2 is increased by nearly 5° by spin-orbit effects. While correlation effects are very important for transition metal compounds, the spin-orbit splitting is of comparable importance. Whether it can be treated as a perturbation in any accurate calculation on Pt compounds is highly questionable.

ACKNOWLEDGEMENTS

The author was supported by NASA grant NCC2-552.

REFERENCES

- [A1] H. Basch and S. Topiol, *J. Chem. Phys.* **71**, 802 (1979).
- [A2] H. Basch, D. Cohen, and S. Topiol, *Isr. J. Chem.* **19**, 233 (1980).
- [A3] S. W. Wang and K. S. Pitzer, *J. Chem. Phys.* **79**, 3851 (1983).
- [A4] A. Gavezzotti, G. F. Tantardini, and M. Simonetta, *Chem. Phys.* **84**, 433 (1986).
- [A5] J. J. Low and W. A. Goddard III, *J. Am. Chem. Soc.* **108**, 6115 (1986).
- [A6] J. J. Low and W. A. Goddard III, *Organometallics* **5**, 610 (1986).
- [A7] E. Poulain, J. Garcia-Prieto, M. E. Ruiz, and O. Novaro, *Int. J. Quantum Chem.* **29**, 1181 (1986).
- [A8] C. M. Rohlfiing, P. J. Hay, and R. L. Martin, *J. Chem. Phys.* **85**, 1447 (1986).
- [A9] K. Balasubramanian, *J. Chem. Phys.* **87**, 2800 (1987).
- [A10] K. Balasubramanian, P. Y. Feng, and M. Z. Liao, *J. Chem. Phys.* **88**, 6955 (1988).
- [A11] H. Nakatsuji, Y. Matsuzaki, and T. Yonezawa, *J. Chem. Phys.* **88**, 5759 (1988).
- [A12] K. Balasubramanian and P. Y. Feng, *J. Chem. Phys.* **92**, 541 (1990).
- [A13] S. Tobisch and G. Rasch, *Chem. Phys. Lett.* **166**, 311 (1990).
- [A14] K. Balasubramanian, *J. Chem. Phys.* **94**, 1253 (1991).
- [A15] M. Sjøvoll, Thesis, Tromsø (1991).
- [A16] O. Gropen, J. Almlöf, and U. Wahlgren, *J. Chem. Phys.* **96**, 8363 (1992).
- [A17] P. A. Christiansen and K. S. Pitzer, *J. Chem. Phys.* **74**, 1162 (1981).
- [A18] K. G. Dyall, *J. Chem. Phys.* **96**, 1210 (1992).
- [A19] K. G. Dyall, *J. Chem. Phys.*, submitted.
- [A20] B. A. Hess, *Phys. Rev. A* **33**, 3742 (1986).
- [A21] R. Samzow and B. A. Hess, *Chem. Phys. Lett.* **184**, 491 (1991).
- [A25] R. D. Cowan and D. C. Griffin, *J. Opt. Soc. Am.* **66**, 1010 (1976).

- [A26] R. L. Martin, *J. Phys. Chem.* **87**, 730 (1983).
- [A27] K. G. Dyall, K. Fægri, Jr., and P. R. Taylor, in *The effects of relativity in atoms, molecules and the solid state*, edited by I. P. Grant, B. Gyorffy, and S. Wilson (Plenum: New York, 1990)
- [A28] K. G. Dyall, K. Fægri, Jr., P. R. Taylor, and H. Partridge, *J. Chem. Phys.* **95**, 2583 (1991).
- [A29] H. Hsu, E. R. Davidson, and R. M. Pitzer, *J. Chem. Phys.* **65**, 609 (1976).
- [A30] K. Fægri, Jr. and R. Manne, *Mol. Phys.* **31**, 1037 (1976).
- [A31] K. Fægri, Technical Note, University of Oslo, 1987.
- [A32] O. Matsuoka and S. Okada, *Chem. Phys. Lett.* **155**, 547 (1989).
- [A33] S. Huzinaga, *J. Chem. Phys.* **42**, 1293 (1965).
- [A34] C. W. Bauschlicher, Jr. and H. Partridge, *Chem. Phys. Lett.* **181**, 129 (1991).
- [A35] K. G. Dyall, I. P. Grant, C. T. Johnson, F. A. Parpia, and E. P. Plummer, *Computer Phys. Commun.* **55**, 425 (1989).
- [A36] MOLECULE-SWEDEN is an electronic structure program system written by J. Almlöf, C. W. Bauschlicher, M. R. A. Blomberg, D. P. Chong, A. Heiberg, S. R. Langhoff, P.-Å. Malmqvist, A. P. Rendell, B. O. Roos, P. E. M. Siegbahn, and P. R. Taylor.
- [A37] INTDER: a program which performs curvilinear transformations between internal and Cartesian coordinates, written by W. D. Allen..
- [A38] S. P. Walch, C. W. Bauschlicher, and S. R. Langhoff, *J. Chem. Phys.* **83**, 5351 (1985).
- [A39] R. Engleman, Jr., *J. Opt. Soc. Am. B* **2**, 1934 (1985).
- [A40] S. F. Boys and F. Bernardi, *Mol. Phys.* **19**, 553 (1970).
- [A41] C. W. Bauschlicher and P. R. Taylor, *Theor. Chim. Acta*, submitted.
- [A42] M. R. A. Blomberg and U. Wahlgren, *Chem. Phys. Lett.* **145**, 393 (1988).
- [A43] J. Almlöf, K. Fægri, Jr., and H. H. Grelland, *Chem. Phys. Lett.* **114**, 53 (1985).

TABLE I. Energy levels in cm^{-1} of atomic Pt from Dirac-Fock calculations on the $(s + d)^{10}$ configuration complex. Column 3 contains energies from diagonalizing the Dirac-Coulomb Hamiltonian in the CSF basis; in column 4 the contribution of the Breit interaction and estimates of quantum electrodynamic corrections have been added to the Dirac-Coulomb Hamiltonian before diagonalization. The configurations are given in hole state notation relative to the fully occupied d and s shells. CSF with weights below 8% have been neglected.

J	E_{DC}	E_{DBQ}	$E_{e\text{zpt}}$	jj -coupling composition	LS -coupling composition
3	0.0	0.0	0.0	100% $[ds]$	100% $[ds]^3 D_3$
4	940.8	495.8	823.7	92% $[d^2]$	96% $[d^2]^3 F_4$
2	1311.7	1204.4	775.9	76% $[ds]$, 19% $[d^2]$	40% $[ds]^3 D_2$, 38% $[ds]^1 D_2$, 16% $[d^2]^1 D_2$
2	6910.2	6567.6	6567.5	47% $[\bar{d}s]$, 39% $[d^2]$	50% $[ds]^3 D_2$, 25% $[d^2]^1 D_2$, 12% $[d^2]^3 F_2$
1	9227.0	8934.7	10132.0	100% $[\bar{d}s]$	100% $[ds]^3 D_1$
3	10286.9	9574.9	10116.8	100% $[\bar{d}d]$	100% $[d^2]^3 F_3$
2	15055.3	14608.8	15501.8	45% $[\bar{d}s]$, 23% $[d^2]$, 19% $[\bar{d}^2]$	46% $[ds]^1 D_2$, 31% $[d^2]^3 F_2$, 10% $[d^2]^3 P_2$
2	17472.7	16787.8	13496.3	69% $[\bar{d}d]$, 17% $[d^2]$, 13% $[\bar{d}^2]$	61% $[d^2]^3 P_2$, 37% $[d^2]^3 F_2$
0	17672.8	17505.5		55% $[d^2]$, 38% $[s^2]$	46% $[d^2]^3 P_0$, 38% $[s^2]^1 S_0$, 17% $[d^2]^1 S_0$
1	22417.9	21716.4	18566.5	100% $[\bar{d}d]$	100% $[d^2]^3 P_1$
0	24350.1	24306.9	6140.0	57% $[s^2]$, 22% $[\bar{d}^2]$, 21% $[d^2]$	57% $[s^2]^1 S_0$, 42% $[d^2]^3 P_0$
4	25053.8	24357.3	21967.1	92% $[\bar{d}d]$	97% $[d^2]^1 G_4$
2	29209.9	28370.8	26638.6	67% $[\bar{d}^2]$, 21% $[\bar{d}d]$	56% $[d^2]^1 D_2$, 18% $[d^2]^3 P_2$, 16% $[d^2]^3 F_2$
0	54687.4	53922.9		70% $[\bar{d}^2]$, 24% $[d^2]$	83% $[d^2]^1 S_0$, 11% $[d^2]^3 P_0$

TABLE II. Properties of the low-lying states of PtH⁺ from NR, PT and DHF calculations on each individual state. Bond lengths r_e are given in Å, harmonic frequencies ω_e and excitation energies T_e in cm⁻¹, dissociation energies D_e in kcal mol⁻¹.

State	r_e	ω_e	T_e	D_e
NR				
$^1\Sigma^+$	1.497	2464	0	9.7
PT				
$^1\Sigma^+$	1.501	2546	0	20.6
$^3\Delta$	1.516	2550	1160	17.3
DHF				
0^+	1.522	2426	0	28.1

TABLE III. Gross Mulliken populations and charges for the NR $^1\Sigma^+$, $^3\Pi$ and $^3\Delta$ states and the DHF 0^+ state of PtH^+ at $r = 3.1a_0$. The populations of the valence σ orbitals and $e_{1/2}$ spinors are displayed for each state, as well as the total populations and the net charge. The f populations on Pt have been omitted, as they make little contribution to the valence populations or to the charges. The charges for Pt are given relative to the d^{10} state of the neutral atom.

	Pt s	Pt p	Pt d	Total	H s	H p	Total
$^1\Sigma^+$							
13 σ	0.074	0.039	1.069	1.186	0.794	0.020	0.814
Charge	-0.074	-0.032	+0.944	+0.834	+0.200	-0.034	+0.166
$^3\Pi$							
13 σ	0.003	0.002	1.715	1.720	0.262	0.018	0.280
14 σ	0.130	0.069	0.108	0.312	0.689	-0.002	0.687
Charge	-0.131	-0.058	+1.187	+0.993	+0.037	-0.030	+0.007
$^3\Delta$							
13 σ	0.009	0.015	1.654	1.680	0.307	0.013	0.320
14 σ	0.178	0.057	0.139	0.376	0.625	-0.002	0.624
Charge	-0.187	-0.067	+1.215	+0.958	+0.063	-0.021	+0.042
0^+							
20 $e_{1/2}$	0.036	0.015	1.671	1.723	0.265	0.012	0.277
21 $e_{1/2}$	0.292	0.054	0.992	1.341	0.646	0.013	0.659
Charge	-0.326	-0.066	+1.344	+0.948	+0.084	-0.032	+0.052

TABLE IV. DHF gross Mulliken populations and integrated spin densities for the spin-orbit components of the valence spinors, total charges and total integrated spin densities of the 0^+ state of PtH^+ at $r = 3.1a_0$. The f populations on Pt have been omitted, as they make little contribution to the valence populations or to the charges. The charges for Pt are given relative to the d^{10} state of the neutral atom.

	Pt				H		Spin	
	$p_{1/2}$	$p_{3/2}$	$d_{3/2}$	$d_{5/2}$	$p_{1/2}$	$p_{3/2}$	α	β
$20e_{1/2}$	0.004	0.011	1.667	0.004	0.000	0.013	0.540	0.460
$21e_{1/2}$	0.026	0.028	0.219	0.772	0.012	0.002	0.576	0.424
Charge	-0.030	-0.036	+0.115	+1.230	-0.011	-0.021		

TABLE V. Properties of the $^1\Sigma^+$ state of PtH^+ from NR and PT calculations as a function of the valence basis. Bond lengths r_e are given in Å, harmonic frequencies ω_e in cm^{-1} , dissociation energies D_e in kcal mol^{-1} .

Basis	r_e	ω_e	D_e
NR			
<i>4s4p4d</i>	1.497	2464	9.66
<i>5s4p4d</i>	1.497	2461	9.67
<i>5s5p4d</i>	1.497	2457	9.69
<i>5s5p5d</i>	1.496	2455	9.72
<i>6s5p5d</i>	1.496	2455	9.70
<i>6s6p5d</i>	1.496	2455	9.68
PT			
<i>4s4p4d</i>	1.492	2306	20.88
<i>5s4p4d</i>	1.496	2551	19.85
<i>5s5p4d</i>	1.500	2548	20.54
<i>5s5p5d</i>	1.501	2546	20.59
<i>6s5p5d</i>	1.502	2536	19.62
<i>6s6p5d</i>	1.503	2537	19.80

TABLE VI. Properties of the low-lying states of PtH from DHF calculations. The states are designated by Ω with the energetic order index in parentheses. Three sets of calculations are described: a 5-state average, a 3-state average and a set of separate calculations on each state. Bond lengths r_e are given in Å, harmonic frequencies ω_e and excitation energies T_e in cm^{-1} , dipole moments in Debye with polarity Pt^+H^- .

State	r_e	ω_e	T_e	μ_e
5-state average				
5/2(1)	1.551	2241	0	
3/2(1)	1.587	2074	3226	
1/2(1)	1.590	2044	3603	
3/2(2)	1.575	2166	11290	
1/2(2)	1.588	2129	11904	
3-state average				
5/2(1)	1.552	2238	0	
3/2(1)	1.587	2078	3226	
1/2(1)	1.583	2085	2882	
Separate				
5/2(1)	1.551	2234	0	2.316
3/2(1)	1.584	2080	3365	2.558
1/2(1)	1.573	2094	2712	2.463

TABLE VII. Properties of the low-lying states of PtH from NR and PT calculations on each individual state. Two PT calculations are shown, with different valence basis sets. Bond lengths r_e are given in Å, harmonic frequencies ω_e and excitation energies T_e in cm^{-1} , dissociation energies D_e in kcal mol^{-1} and dipole moments μ_e in Debye. The NR D_e is given relative to Pt d^{10} ; the PT D_e is given relative to Pt d^9s . RHM: ECP(nc/18) UHF results of Rohlfing *et al.*, ref A8.

State	r_e	ω_e	T_e	D_e	μ_e
NR					
$^2\Sigma^+$	1.652	1754	0	14.2	2.919
PT 4s4p4d					
$^2\Delta$	1.579	2035	0	38.8	
$^2\Pi$	1.655	1815	3229	29.6	
$^2\Sigma^+$	1.575	1960	650	36.9	
PT 5s5p5d					
$^2\Delta$	1.593	2014	246	37.9	2.932
$^2\Pi$	1.670	1811	3333	29.1	3.472
$^2\Sigma^+$	1.576	1949	0	38.6	3.234
RHM					
$^2\Delta$	1.539	2292	0	48.2	
$^2\Pi$	1.597	2050	4597	35.0	
$^2\Sigma^+$	1.551	2194	1371	44.5	

TABLE VIII. Mulliken population analysis from DHF calculations on the lowest $\omega = 5/2$, $3/2$ and $1/2$ states of PtH at $r = 3.0a_0$. The populations of the valence $e_{1/2}$ spinors are displayed for each state, as well as the total populations and the net charge. The f populations on Pt have been omitted, as they make little contribution to the valence populations or to the charges. The atomic charges for Pt are given relative to the d^9s state.

	Pt				H		
	<i>s</i>	<i>p</i>	<i>d</i>	Total	<i>s</i>	<i>p</i>	Total
5/2							
20 $e_{1/2}$	0.045	0.034	1.332	1.411	0.576	0.012	0.589
21 $e_{1/2}$	0.033	0.019	1.727	1.780	0.212	0.008	0.220
22 $e_{1/2}$	1.024	0.004	0.594	1.625	0.375	0.000	0.375
Charge	-0.100	-0.053	+0.355	+0.199	-0.171	-0.028	-0.199
3/2							
20 $e_{1/2}$	0.042	0.024	1.347	1.411	0.575	0.014	0.589
21 $e_{1/2}$	0.037	0.018	1.701	1.756	0.234	0.010	0.244
22 $e_{1/2}$	0.969	0.014	0.624	1.612	0.388	0.000	0.388
Charge	-0.045	-0.047	+0.334	+0.240	-0.208	-0.032	-0.240
1/2							
20 $e_{1/2}$	0.107	0.024	1.236	1.367	0.620	0.013	0.633
21 $e_{1/2}$	0.305	0.034	1.129	1.471	0.522	0.007	0.529
22 $e_{1/2}$	0.309	0.000	0.644	0.952	0.047	0.001	0.048
Charge	+0.282	-0.053	+0.001	+0.227	-0.197	-0.031	-0.227

TABLE IX. Nonrelativistic gross Mulliken populations and charges for the ${}^2\Delta$, ${}^2\Pi$ and ${}^2\Sigma^+$ states of PtH at $r = 3.0a_0$. The populations of the valence σ orbitals are displayed for each state, as well as the total populations and the net charge. The f populations on Pt have been omitted, as they make little contribution to the valence populations or to the charges. The atomic charges for Pt are given relative to the d^9s state.

	Pt				H		
	<i>s</i>	<i>p</i>	<i>d</i>	Total	<i>s</i>	<i>p</i>	Total
${}^2\Delta$							
13 σ	0.012	0.020	1.561	1.593	0.399	0.009	0.407
14 σ	0.760	0.088	0.284	1.136	0.866	-0.003	0.863
Charge	+0.229	-0.106	+0.167	+0.285	-0.269	-0.016	-0.285
${}^2\Pi$							
13 σ	0.009	0.007	1.593	1.606	0.382	0.012	0.394
14 σ	0.669	0.121	0.293	1.091	0.912	-0.003	0.909
Charge	+0.321	-0.115	+0.157	+0.356	-0.333	-0.023	+0.356
${}^2\Sigma^+$							
13 σ	0.089	0.034	0.960	1.085	0.904	0.011	0.915
14 σ	0.236	0.042	0.433	0.713	0.287	0.000	0.287
Charge	+0.676	-0.069	-0.379	+0.226	-0.200	-0.026	-0.226

TABLE X. Mulliken population analysis of the atomic spin-orbit components of the valence spinors for the lowest $\omega = 5/2, 3/2$ and $1/2$ states of PtH at $r = 3.0a_0$. The f populations on Pt have been omitted, as they make little contribution to the valence populations or to the charges. The charges for Pt are given relative to the $d_{3/2}^4 d_{5/2}^5 s_{1/2}^1$ state of the atom.

	Pt				H	
	$p_{1/2}$	$p_{3/2}$	$d_{3/2}$	$d_{5/2}$	$p_{1/2}$	$p_{3/2}$
5/2						
20 $e_{1/2}$	0.013	0.021	1.142	0.190	0.001	0.011
21 $e_{1/2}$	0.013	0.006	0.656	1.071	0.009	-0.001
22 $e_{1/2}$	0.003	0.001	0.104	0.491	0.000	0.000
Charge	-0.028	-0.025	+0.100	+0.255	-0.009	-0.019
3/2						
20 $e_{1/2}$	0.009	0.015	1.120	0.227	0.001	0.013
21 $e_{1/2}$	0.014	0.004	0.718	0.983	0.011	-0.001
22 $e_{1/2}$	0.007	0.008	0.078	0.546	0.000	0.000
Charge	-0.028	-0.019	+0.141	+0.193	-0.013	-0.019
1/2						
20 $e_{1/2}$	0.008	0.017	1.200	0.036	0.000	0.013
21 $e_{1/2}$	0.022	0.012	0.677	0.452	0.008	-0.001
22 $e_{1/2}$	-0.001	0.000	0.032	1.256	0.002	0.000
Charge	-0.028	-0.025	+0.109	-0.108	-0.009	-0.021

TABLE XI. DHF integrated spin densities for the valence spinors (Kramers pairs) of the lowest $\omega = 5/2, 3/2$ and $1/2$ states of PtH at $r = 3.0a_0$. The values shown are for the $e_{1/2}, e_{-3/2}$ and $e_{5/2}$ spinors. The time-reversed spinors $e_{-1/2}, e_{3/2}$ and $e_{-5/2}$ have the same densities with opposite spin. The densities represent the occupation number of the orbital whose symmetry type given at the head of the column. The sum is taken over spin for all occupied valence spinors. (The core sums give the expected integer occupation numbers.)

	$\sigma(\alpha)$	$\pi(\beta)$	$\delta(\alpha)$
5/2			
20 $e_{1/2}$	0.847	0.153	
21 $e_{1/2}$	0.175	0.825	
22 $e_{1/2}$	0.981	0.019	
11 $e_{-3/2}$		0.875	0.125
12 $e_{-3/2}$		0.125	0.875
5 $e_{5/2}$			1.000
Sum	4.006	3.994	3.000
3/2			
20 $e_{1/2}$	0.865	0.135	
21 $e_{1/2}$	0.172	0.828	
22 $e_{1/2}$	0.968	0.032	
11 $e_{-3/2}$		0.584	0.416
12 $e_{-3/2}$		0.416	0.584
5 $e_{5/2}$			1.000
Sum	4.010	3.574	3.416
1/2			
20 $e_{1/2}$	0.739	0.261	
21 $e_{1/2}$	0.430	0.570	
22 $e_{1/2}$	0.836	0.164	
11 $e_{-3/2}$		0.553	0.447
12 $e_{-3/2}$		0.447	0.553
5 $e_{5/2}$			1.000
Sum	3.174	3.826	4.000

TABLE XII. Bond length, r_e , in Å, bond angle, θ_e , in degrees, dipole moment, μ_e , in Debye and energy of decomposition into Pt and H₂, ΔE , in kcal/mol into Pt and H₂ of PtH₂.

	r_e	θ_e	μ_e	ΔE
PT	1.534	83.3		13.3
PVP				
DHF	1.525	88.1	2.503	35.1

Edit for length

SUMMARY

The investigation into the appearance of intruder states from the negative continuum when some of the two-electron integrals involving the small component of the wave function were omitted has been completed and published [1]. The work shows that provided all integrals involving core contracted functions in an atomic general contraction are included, or that the core functions are radially localized, meaningful results are obtained and intruder states do not appear. Reprints of the paper are attached.

In the area of program development, the Dirac-Hartree-Fock (DHF) program for closed-shell polyatomic molecules has been extended to permit Kramers-restricted open-shell DHF calculations with one electron in an open shell or one hole in a closed shell, or state-averaged DHF calculations over several particle or hole doublet states. Code for two open shells is still being tested, as is code for limited MCSCF, for situations where the ground state at the DHF level cannot be described by a single determinant, but is a linear combination of a few determinants related by double excitations from one Kramers pair into another. One application of the open-shell code was to the KO molecule [2]. Preprints of this paper are attached.

Another major area of program development which is under development is the transformation of integrals from the scalar basis in which they are generated to the 2-spinor basis employed in parts of the DHF program, and thence to supermatrix form. The reason for these developments is that the DHF program, while written efficiently for the circumstances under which it was expected to be used, is not the most efficient implementation possible. The code was

originally developed under the assumption that disk space would not be available to sort and transform the integrals, and therefore the unordered integrals would have to be used in the construction of the Fock matrix. With the experience gained over the past year, particularly concerning the omission of small component integrals, and with the increase in availability of disk space, it is now possible to consider transforming the integrals. The use of ordered integrals, either in the scalar basis or in the 2-spinor basis, would considerably speed up the construction of the Fock matrix, and even more so if supermatrices were constructed. Furthermore, in order to proceed beyond the SCF level and include electron correlation it is necessary to transform the integrals to the molecular 4-spinor basis. Therefore, a considerable amount of effort has been spent on analyzing the integral ordering and transformation for the DHF problem. Much of this work was used in preparation for the NATO Advanced Summer Institute in Vancouver, BC, in August 1992.

The work of assessing the reliability of the relativistic effective core potentials (RECPs) available in the literature has been continued with calculations on the group IV monoxides. The perturbation of the metal atom provided by oxygen is expected to be larger than that provided by hydrogen and thus provide a better test of the quality of the RECPs. The results of this study have been submitted for publication, and preprints are attached [3].

Calculations on the platinum hydrides PtH , PtH^+ and PtH_2 have been carried out at the nonrelativistic (NR), perturbation theory (PT) and DHF levels. The DHF calculations employed the new open-shell code described above. Geometries, dipole moments, harmonic frequencies, infrared intensities and disso-

ciation energies have been calculated. For purposes of separating spin-orbit effects from the non-fine-structure effects and for determining the validity of the first-order PT approximation, it is proposed to include in the results for the platinum hydrides calculations with the spin-free no-pair code of Hess [4]. A preliminary draft of the paper without these calculations is attached. These results were presented at the West Coast Theoretical Chemistry Conference, held in May 1992 at Pacific Northwest Laboratory.

REFERENCES

- [1] K. G. Dyall, Chem. Phys. Lett. 196, 178 (1992).
- [2] C. W. Bauschlicher, H. Partridge and K. G. Dyall, Chem. Phys. Lett., in press.
- [3] K. G. Dyall, J. Chem. Phys., submitted.
- [4] B. A. Hess, Phys. Rev. A 33, 3742 (1986).

